BOR Papers in Press. Published on June 17, 2015 as DOI:10.1095/biolreprod.114.127423

Procaine Induces Cytokinesis in Horse Oocytes via a pH-Dependent Mechanism[1]

Running title: PROCAINE INDUCES CYTOKINESIS IN EQUINE OOCYTES

Bart Leemans[3], Bart M. Gadella[4,5], Tom A.E. Stout[4,6], Sonia Heras[3], Katrien Smits[3], Minerva Ferrer-Buitrago[7], Eline Claes[3], Björn Heindryckx[7], Winnok H. De Vos[8,9], Hilde Nelis[3], Maarten Hoogewijs[3], Ann Van Soom[2,3]

[3]Department of Reproduction, Obstetrics and Herd Health, Faculty of Veterinary Medicine, Ghent University, Belgium
[4]Department of Farm Animal Health, Faculty of Veterinary Medicine, Utrecht University, The Netherlands
[5]Department of Biochemistry and Cell Biology, Faculty of Veterinary Medicine, Utrecht University, The Netherlands
[6]Deparment of Equine Sciences, Faculty of Veterinary Medicine, Utrecht University, The Netherlands
[7]Department for Reproductive Medicine, Ghent University Hospital, Ghent University, Belgium
[8]Department Veterinary Sciences, Faculty of Pharmaceutical, Biomedical and Veterinary Sciences, Antwerp University, Belgium
[9]Department Molecular Biotechnology, Cell Systems and Cellular Imaging, Faculty of Bioscience Engineering, Ghent University, Belgium

[1]Supported by the Agency for Innovation in Science and Technology (IWT-Flanders; grant number 101521).

[2]Correspondence: Ann Van Soom, Salisburylaan 133, 9820 Merelbeke, Belgium. E-mail: Ann.VanSoom@ugent.be

ABSTRACT

Co-incubating equine gametes in the presence of procaine has been reported to facilitate *in vitro* fertilization, with cleavage rates exceeding 60%. We report that, while procaine does trigger sperm hyperactivation, it independently induces cleavage of equine oocytes. First, we found that procaine (1-5 mM) did not facilitate stallion sperm penetration of equine oocytes, but instead induced sperm-independent oocyte cytokinesis in the absence of the second polar body extrusion. Indeed, 56 ± 4% of oocytes cleaved within 2.5 d of exposure to 2.5 mM procaine, irrespective of sperm presence. However, the cleaved oocytes did not develop beyond 8-16 cells, and the daughter cells either lacked nuclei or contained aberrant, condensed DNA fragments. By contrast, intra-cytoplasmic sperm injection (ICSI) was followed by second polar body extrusion and formation of normal blastocysts. Moreover, neither the calcium oscillations detectable using fura-2 AM staining nor the cortical granule reaction visualized by LCA-FITC staining, after oocyte activation induced by ICSI or ionomycin treatment, were detected after exposing oocytes to 2.5 mM procaine. Instead, procaine initiated an ooplasmic alkalinization, detectable by BCECF-AM staining that was not observed after other treatments. This alkalinization was followed, after an additional 18 h incubation, by cortical F-actin depolymerization, as demonstrated by reduced actin phalloidin-FITC staining intensity, that resembled preparation for cytokinesis in ICSI-fertilized zygotes. Overall, we conclude that procaine induces cytokinesis in equine oocytes accompanied by aberrant chromatin condensation and division; this explains why embryos produced after exposing equine oocytes to procaine fail to develop beyond the 8-16 cell stage.

Summary sentence: Procaine does not induce penetration of equine oocytes by activating stallion sperm, but instead stimulates cytokinesis of the oocytes via a pH mediated depolymerization of cortical F-actin.

Keywords: *procaine, IVF, cytokinesis, pH, F-actin, equids*

INTRODUCTION

The birth of two foals produced after *in vitro* fertilization (IVF) of *in vivo* matured equine oocytes was reported in 1991 [1, 2]. Unfortunately, subsequent attempts to establish a repeatable protocol for conventional IVF in horses have not been successful [3, 4], and it has been suggested that the primary deficit is the inability to adequately induce capacitation of stallion spermatozoa *in vitro*. More specifically, the absence of hyperactivated sperm motility under standard *in vitro* capacitation conditions has been proposed as the main reason why *in vitro* fertilization fails in the horse [5]. In 2009, McPartlin et al. [6] reported promising equine IVF results after including procaine in the co-incubation medium. The procaine induced hyperactivated motility in stallion spermatozoa, and this was concluded to be responsible for the high cleavage rates observed in the incubated oocytes. An additional important step in the capacitation process, protein tyrosine phosphorylation, was shown to be provoked by incubating stallion spermatozoa in air, and to be independent of the exposure to procaine [6, 7]. Most importantly, approximately 60% of mature (MII) oocytes developed two pronuclei during a 24 h culture subsequent to 18 h co-incubation with procaine-activated sperm. Embryo development was reported up to the 8-cell stage (day 3). More recently, Ambruosi et al. (2013) similarly reported that almost 40% of horse oocytes exposed to sperm and procaine formed two pronuclei after 24 h incubation in identical hyperactivation conditions [8].

Procaine is a local anesthetic known to induce a neuromuscular block and to increase the neuromuscular responses to non-depolarizing muscle relaxants, primarily via actions on the voltage-gated sodium channel [9]. The hyperactivation of sperm motility by procaine (guinea pig, [10]; horse, [6, 11, 12]) has, in the horse, been associated with a moderate increase in intracellular pH, an obligatory step in initiating pH-gated calcium influx through CatSper channels [13]. Surprisingly, procaine-induced hyperactivated motility was not dependent on external calcium in either stallion [12] or guinea pig [10] spermatozoa, supporting the hypothesis that the calcium is mobilized from internal calcium stores, which contrasts to what is thought to happen during physiological induction of hyperactivated sperm motility [14, 15].

The two published studies on the effects of procaine on horse IVF [6, 8] used the same approach, i.e. they exposed both oocytes and spermatozoa simultaneously to procaine. Therefore, a concurrent effect of procaine on oocyte activation cannot be excluded. Oocytes require a rise in cytoplasmic calcium after fertilization or parthenogenetic activation to resume meiosis and embark on embryonic development. During gamete fusion, a sperm-specific phospholipase C zeta (PLCζ) is introduced into the oocyte, and is a key factor in inducing an inositol triphosphate (IP3) mediated calcium release from intracellular stores (calcium oscillations; mouse [16], human [17]). Various methods have been employed to induce artificial calcium oscillations in mammalian oocytes *in vitro* and thereby provoke oocyte activation and embryo development. Electrical pulses [18], calcium ionophore [19] and strontium [20] are typically used as parthenogenetic agents, and it has been demonstrated that electrical pulses and calcium ionophore generate a single calcium elevation whereas multiple calcium oscillations are induced by normal fertilization or strontium [20]. Moreover, there is some evidence that procaine is able to disregulate cytoplasmic calcium rise(s) in female gametes. In pig [21, 22] and cattle [23, 24] oocytes, the calcium rise could be inhibited by injecting procaine into the cytoplasm. Further downstream in the oocyte activation pathway, the calcium rise triggers the cortical granule reaction. In many mammalian species, including the horse [25], cortical granule accumulation at the periphery of the oocyte cytoplasm (horse, [25]; pig, [26, 27]) is indicative of cytoplasmic maturation; moreover, these granules are extruded into the perivitelline space after the onset of calcium oscillations during oocyte activation [25].

Another effect of procaine on female gametes has been described in the sea urchin, namely that procaine and other weak bases provoke an elevation in cytoplasmic pH [28, 29] that, in turn, induces cortical F-actin turnover [29] as part of the dramatic changes that the cytoskeleton of a mature oocyte needs to undergo in response to activation [28]. In particular, the total amount of F-actin first increases and subsequently decreases to allow cytokinesis [30].

Since the inclusion of procaine in equine *in vitro* fertilization media has been shown to induce oocyte cleavage but did not result in blastocyst formation, the aim of this study was to investigate the effect of procaine on equine oocyte activation, cytokinesis and fertilization. The direct effect of procaine on (1) sperm penetration through the zona pellucida, (2) the activation of the oocyte's cortical granule reaction, (3) the presence and arrangement of chromatin in the cleavage products, (4) changes in cytoplasmic calcium and pH in oocytes, (5) and F-actin distribution in oocytes, were assessed. The resulting data help explain why including procaine in equine IVF media resulted in high oocyte cleavage rates without development to the blastocyst stage.

MATERIALS AND METHODS

Chemicals and Reagents

Alexa Fluor 488-conjugated goat anti-mouse antibody, Hoechst 33342, MitoTracker Green FM and BCECF-acetoxymethyl (AM) ester were obtained from Molecular Probes (Ghent, Belgium). Monoclonal 4G10 Platinum anti-phosphotyrosine mouse antibodies were purchased from Millipore (Overijse, Belgium). Fura-2 AM ester was obtained from Invitrogen (Life Technologies, Merelbeke, Belgium) and LCA-FITC was purchased from Labconsult SPRL (Vector Labs, Brussels, Belgium). Dimethylsulfoxide (DMSO), fatty acid-free bovine serum albumin (A9418; cell culture tested), lacmoid, phalloidin-FITC, triton X-100, tween, pronase from *streptomyces griseus* and all other chemicals not otherwise listed were obtained from Sigma-Aldrich (Bornem, Belgium).

Semen Collection and Preparation

Semen was collected from three adult stallions of proven good fertility using a Colorado model artificial vagina (Animal Reproduction Systems; Chino, CA, USA). The raw ejaculate was filtered through gauze to remove the gel fraction and any debris, before visual evaluation of sperm motility by light microscopy (200x) on a heated stage at 37°C; if the motility was acceptable (>65% motile), the semen was immediately transported to the laboratory for further processing. One ml of fresh semen with a concentration of 100 to 300 x 10^6 spermatozoa/ml was washed using a 45/90% Percoll gradient [31, 32]. Next, the sperm pellet was washed once with non-capacitating medium (100 mM NaCl, 4.7 mM KCl, 1.2 mM $MgCl_2$, 5.5 mM glucose, 22 mM HEPES, 2.4 mM sodium lactate and 1.0 mM pyruvic acid; pH=7.4 and 280-300 mOsm/kg; [7]). Each experiment was performed using one ejaculate from each of the three stallions. The study was approved by the Ethics Committee of the Faculty of Veterinary Medicine of Ghent University (EC2013/175 and EC2013/176).

For the sperm penetration experiments, spermatozoa were labelled with MitoTracker Green FM before further processing. Briefly, 200 nM MitoTracker Green FM dissolved in 0.025% DMSO was added to the Percoll washed sperm suspension (100 x 10^6 spermatozoa/ml) diluted in 10 ml non-capacitating medium. After 30 min incubation at 37 °C, the sperm suspension was washed twice in 10 ml non-capacitating medium (600g; 5 min).

Sperm Capacitation/ Hyperactivation

To provide conditions supportive of sperm capacitation, non-capacitating medium was modified by replacing the sodium lactate with 2.4 mM calcium lactate and adding 25 mM $NaHCO_3$ and 7 mg/ml BSA (pH=7.4; 280-300 mOsm/kg; osmolality was adjusted by graduated addition of the NaCl); this medium

was pre-equilibrated for at least 2 h in a humidified atmosphere containing 5% CO_2 at 38.5 °C and is further referred to as capacitating medium (adapted from McPartlin et al. [7]). The washed sperm pellet was diluted to a concentration of 10 x 10^6 spermatozoa/ml with capacitating medium. After 6 h pre-incubation in humidified air at 38.5°C, hyperactivated motility was induced by resuspending the spermatozoa in capacitating medium supplemented with either 0, 1, 2.5 or 5 mM procaine hydrochloride (Sigma-Aldrich, Bornem, Belgium) at a final concentration of 1 x 10^6 spermatozoa/ml [6]. More precisely, a stock of 10 mM procaine hydrochloride dissolved in capacitating medium was pre-equilibrated for at least 2 h in a humidified atmosphere containing 5% CO_2 at 38.5°C to restore the pH to the physiological range (7.2 - 7.4). Moreover, various procaine concentrations (0, 1, 2.5 and 5 mM) were prepared by diluting the stock solution with the required amount of equilibrated capacitating medium. In this way the pH of all incubation media was adjusted to 7.2-7.4.

Oocyte Maturation

Ovaries were collected from slaughtered mares (Euro Meat Group, Moeskroen, Belgium). Within 4 h after slaughter, all follicles larger than 5 mm were aspirated using a 16 gauge needle attached to a vacuum pump (~100 mm Hg), scraped with the aspirating needle and flushed with phosphate buffered saline (DPBS) containing 25 IU/ml heparin. A maximum of 30 cumulus-oocyte complexes (COCs) were transferred to 500 µl Dulbecco's Modified Eagle Medium Nutrient Mixture F-12 (DMEM-F12) based maturation medium [33] and placed in an incubator at 38.2°C in a humidified atmosphere of 5% CO_2-in-air for 28 h. After maturation, COCs were partially or completely denuded by gentle pipetting in 0.05% bovine hyaluronidase diluted in 4-(2-hydroxyethyl)-1-piperazine ethanesulfonic acid (HEPES) buffered DMEM-F12 medium. Degenerated oocytes were excluded from subsequent experiments. Only completely denuded oocytes with an extruded polar body were used for piezo drill intra-cytoplasmic sperm injection (ICSI) or parthenogenetic activation by ionomycin treatment, whereas all non-degenerated oocytes were used for IVF with the assumption that an extruded polar body was present since it could not be visualized in partially cumulus-enclosed oocytes.

In Vitro Fertilization/Oocyte Activation/Cytokinesis in the Presence of Procaine

Equine IVF was performed in the presence of 0, 1, 2.5 or 5 mM procaine hydrochloride, as described by McPartlin et al. [6]. As previously indicated, sperm was incubated at 10 x 10^6 spermatozoa/ml in capacitating medium for 6 h and then diluted to 1 x 10^6 spermatozoa/ml in procaine containing capacitating medium to achieve final concentrations of 0, 1, 2.5 or 5 mM procaine (medium pH=7.2-7.4; previously adjusted by incubation in an atmosphere containing 5% CO_2). One hundred µl droplets of these sperm suspensions were pipetted into petri dishes and covered with 5% CO_2 equilibrated mineral oil. Five completely or partially denuded mature oocytes were then transferred to each medium droplet, and the petri dishes were incubated at 38.2°C in 5% CO_2 in humidified air. After 18 h of co-incubation, partially denuded oocytes were fully denuded by gentle pipetting in 0.05% bovine hyaluronidase in HEPES buffered DMEM/F12. Subsequently, oocytes were checked for sperm penetration or cultured for an additional 6 h to assess oocyte nuclear configuration and second polar body formation; or 2.5 days in groups of 5 oocytes per 5 µl droplet of DMEM-F12 with 10% fetal calf serum, at 38.5°C in a humidified atmosphere of 5% CO_2, 5% O_2 and 90% N_2. The presumptive embryos were fixed at different developmental stages (zygote, 2-cell, 4-8 cell, 8-16 cell) to assess nuclear configuration, second polar body formation and developmental stage. Oocytes were incubated in similar procaine-containing media in the absence of sperm.

Parthenogenetic Activation by Ionomycin

Parthenogenetically activated equine oocytes were used as negative controls for sperm penetration and its role in calcium dependent oocyte activation, including second polar body formation. The protocol was performed as described by Heras et al. ([34]; based on K. Hinrichs, personal communication). Briefly, cumulus-denuded mature oocytes were incubated for 4 min in 5 µM ionomycin diluted in non-capacitating medium on a heated stage (37°C). After washing five times in wash medium (0.5% BSA in

DPBS), oocytes were incubated for 30 min in non-capacitating medium and then transferred to 2 mM 6-(dimethylamino)purine dissolved in DMEM/F12 medium. After 4 h incubation, the oocytes were washed 5 times with wash medium and once with DMEM/F12. The parthenogenetically activated oocytes were cultured in groups of 5 in 5 µl droplets of DMEM-F12 with 10% fetal calf serum at 38.5°C in a humidified atmosphere of 5% CO_2, 5% O_2 and 90% N_2.

ICSI

ICSI zygotes were used as a positive control for sperm penetration, second polar body formation, embryonic development up to the blastocyst stage (7-9 days after ICSI), DNA configuration, the cytoplasmic calcium response to fertilization and F-actin redistribution. ICSI was performed as described by Smits et al. [35]. In brief, in preparation for ICSI the oocytes were held in (HEPES) buffered DMEM/F12 medium, and the sperm in 9% polyvinylpyrrolidone in PBS. All manipulations were performed on the heated stage (38.5 °C) of an inverted microscope. A progressively motile sperm was immobilized and subsequently injected into the cytoplasm of a mature oocyte using a piezo drill (Prime Tech, Ibaraki, Japan). The injected oocytes were cultured in groups of 5 in 5 µl droplets of DMEM-F12 with 10% fetal calf serum at 38.5°C in a humidified atmosphere of 5% CO_2, 5% O_2 and 90% N_2.

Quantification of Tail-Associated Protein Tyrosine Phosphorylation

Assessment of protein tyrosine phosphorylation was performed as described by Leemans et al. [36]. Briefly, after 6 h of incubating pre-labelled (200 nM MitoTracker Green FM in 0.025% DMSO) or non-labelled sperm in various concentrations of procaine (0, 1, 2.5, 5 mM) and atmospheric conditions (5% CO_2 or air), sperm suspensions were washed twice and fixed in 4% paraformaldehyde in DPBS at room temperature for 15 min. The fixative was removed by three centrifugation steps using DPBS (600g for 5 min). The washed spermatozoa were subsequently incubated in 0.1% Triton X-100 in DPBS for 10 min at room temperature to ensure complete permeabilization of the membranes. The permeabilized spermatozoa were then incubated in blocking buffer (DPBS containing 1% BSA) for 10 min at room temperature. Next, the spermatozoa were incubated overnight at 4°C in buffer containing 0.1% BSA and the mouse monoclonal 4G10 Platinum IgG_{2b} protein anti-phosphotyrosine antibody (diluted 1:500). After incubation, unbound antibody was removed by washing the spermatozoa twice with 1 ml of DPBS containing 0.1% BSA (600g for 5 min). The spermatozoa were then stained with a monoclonal goat anti-mouse antibody conjugated to Alexa Fluor 488 (Invitrogen, Molecular Probes, Ghent, Belgium) for 1h at room temperature. After immunolabelling, the non-bound antibody conjugates were removed by washing three times with DPBS containing 0.1% BSA, and once using DPBS (600g for 5 min). The immunolabelled spermatozoa were mounted on glass slides under a cover slip and sealed with nail polish. The proportion of spermatozoa with green fluorescent tails among the total sperm population (with Hoechst 33342 fluorescent heads) was determined by randomly scoring 200 spermatozoa. Samples were examined using a Leica DMR microscope equipped with a mercury lamp and appropriate filters, at a magnification of 400x.

Sperm Penetration, DNA Configuration, and Embryonic Development

Oocytes and zygotes were fixed at different developmental stages in 4% paraformaldehyde in DPBS at room temperature for 1 h. The fixative was removed by washing the oocytes twice in wash medium. Next, the fixed oocytes were incubated in a 3.2 µM Hoechst 33342 solution in wash medium for 10 min at room temperature. The oocytes were then washed 4 times in wash medium and mounted on siliconized glass slides (Marienfeld, Germany) using 1,4-Diazabicyclo[2,2,2]octane (DABCO) as antifade, and sealed with nail polish. Excessive pressure from the cover slip was prevented by placing a few droplets of vaseline on the microscope slides prior to mounting. Starting from the incubation in Hoechst 33342, oocytes were shielded from the light to prevent premature fading. Mounted slides were kept at 4°C in the dark until evaluation. The presence of a MitoTracker Green FM positive sperm tail in the oocyte cytoplasm indicated sperm penetration through the zona pellucida (fertilization) while the Hoechst stain visualized the DNA of both the oocyte and the spermatozoa. The presence of a second polar body containing

condensed DNA was also determined using both Hoechst staining and a fluorescent miscroscope and light microscopy, because it is a hall mark of oocyte activation during fertilization and signals the completion of the second meiotic division of the maternal chromatin. After 2.5 d in culture, the ability of equine oocytes/zygotes to undergo nuclear duplication and cell cleavage was assessed. Alternatively, oocyte degeneration was apparent if the oocytes showed an irregular oolemma or shape.

To confirm the validity of the MitoTracker Green FM labelled sperm-oocyte penetration experiments, *in vitro* fertilization was alternatively performed using unlabelled spermatozoa with sperm-penetration assessed by post-fixation lacmoid staining, as described by Martinez et al. [37]. Briefly, after IVF incubation and removal of the cumulus cells, denuded oocytes were mounted on a glass slide and fixed with acetic alcohol (acetic acid to ethanol, 1:3 v:v) for at least 24 h. The fixed oocytes were stained with 1% (w:v) lacmoid in acetic acid. The stained oocytes were immediately evaluated under a phase contrast microscope at x400 magnification. Oocytes were considered to have been penetrated (fertilized) when at least one sperm tail was visible within the oocyte cytoplasm and the DNA of both the oocyte and the spermatozoa could be visualized. The presence of a second polar body was also examined.

Calcium Oscillation Pattern Analysis

The possibility that 2.5 mM procaine induced oocyte activation by triggering calcium influx was investigated by imaging calcium oscillations. The calcium oscillation patterns were compared to those for oocytes activated parthenogenetically using ionomycin, and for oocytes fertilized by ICSI. The protocol was based on that described by Nikiforaki et al. [38]. Briefly, morphologically normal MII stage equine oocytes were loaded with 7.5 µM of the ratiometric calcium sensitive dye fura-2 acetoxymethyl (AM) ester in non-capacitating medium at 38.5 °C in air for 20 min, and then washed repeatedly in non-capacitating medium. The oocytes were then transferred to a 20 µl droplet of capacitating medium containing 2.5 mM procaine or 5 µM ionomycin, or subjected to ICSI in the absence of either activator, and incubated under equilibrated mineral oil on a 35 mm diameter glass bottom dish (MatTek Corp., cat.no. P35G-0P 14-C, Ashland, USA).

Calcium imaging was performed on the pre-heated stage (38.5 °C) of an inverted epifluorescence microscope (TH4-200, Olympus Soft Imaging Solutions GmBH, Belgium) equipped with a 10× objective (100x magnification) and UV light provided by a 75W Xenon arc lamp and modulated by neutral density filters. Recording cytoplasmic calcium began immediately after the exposure of oocytes to procaine or ionomycin, and within 40 min after ICSI. In the procaine and ionomycin groups, fluorescence measurements were made every 10 s for 6 h with a filter switch that provided excitation alternating between 340 and 380 nm; no illumination was applied between measurements. Similar measurements were performed every 30 s for 16 h in oocytes fertilized by ICSI. The concentration of free intracellular calcium was assumed to be proportional to the ratio of fluorescence at 340/380 (expressed in arbitrary units, AU). Baseline fluorescence was then set to ratio = 1. The microscope was equipped with an Okolabs stage micro-environment chamber enclosed in a CO_2 microscope cage incubator so that all measurements were conducted at 37 °C in the presence of 6% CO_2. Oocytes that did not show any calcium oscillations in the ionomycin group were considered non-activated while, in the ICSI group, non-reactive oocytes were considered non-fertilized. In these two groups, only oocytes that showed a calcium signal were included in subsequent analysis of calcium oscillation patterns.

Distribution of the Cortical Granules

The protocol for assessing cortical granule distribution was adapted from Carneiro et al. [25]. Briefly, the zona pellucida (ZP) was first removed by incubating the denuded oocytes for 2-5 min at 38.5°C in 0.3% pronase from streptomyces griseus in HEPES-buffered TCM-199 with Hank's salts. The oocytes were then fixed in 4% paraformaldehyde in DPBS for 30 min at room temperature. Next, the oocytes were washed twice in wash medium before being incubated for 2 h in blocking solution (0.1% BSA, 0.75% glycine and 0.2% NaN_3 in DPBS) at room temperature. After this step, oocytes were incubated for 1 h at

room temperature in permeabilization solution (0.5% Triton X-100 and 0.05% Tween in blocking solution). Permeabilized oocytes were washed twice in wash medium before labelling the cortical granules by incubation for 15 min at room temperature in 10 µg/ml fluorescein isothiocyanate-labelled *Lens culinaris* agglutinin (FITC-LCA) in blocking solution. To verify the nuclear status, the chromatin was counterstained with 3.2 mM Hoechst 33342 in wash medium for 10 min at room temperature. Subsequently, the oocytes were mounted on glass microscope slides as described above. LCA labelled oocytes were further divided into two categories based on the distribution of the cortical granules: (1) clearly visible cortical granules at the periphery of the ooplasm, indicating oocyte cytoplasmic maturation and (2) absence of cortical granules in the oocyte cytoplasm, indicating cortical granule exocytosis.

Assessing Cytoplasmic pH of Procaine Activated Oocytes

Mature oocytes were washed twice using non-capacitating medium and stained with 5 µM of the pH-sensitive dye BCECF-AM in non-capacitating medium by incubation at 38.5°C for 30 min. The extracellular dye was then removed by washing the oocytes twice in non-capacitating medium, and the washed oocytes were transferred to capacitating medium in which they were incubated for a further 20 min to allow de-esterification of the BCECF-AM. Subsequently, the BCECF signal was measured in oocytes mounted on glass slides after 0, 1, 3 and 6 h incubation in capacitating medium containing 0, 1, 2.5, 5 and 10 mM procaine.

Imaging of oocyte cytoplasmic pH was performed on the pre-heated stage (38.5°C) of a fluorescence microscope (Leica DM 5500 B microscope; Leica Microsystems GmbH; Wetzlar, Germany) equipped with a 10× objective (100x magnification) and with UV light provided by a 120 W Hg lamp and modulated by neutral density filters. Recording of cytoplasmic pH was performed using a filter switch that provided excitation alternating between 440 and 490 nm. The cytoplasmic pH was proportional to the ratio of fluorescence at 440/490 (expressed in arbitrary units, AU). Baseline fluorescence was then set to ratio = 1.

To make representative images, the fluorescent signal for BCECF-AM labelled oocytes was acquired after 1 h incubation in various procaine concentrations and loaded into the Image Database program (Leica, Van Hopplynus N.V., Brussel, Belgium). We set the baseline pH as that observed in 0 mM procaine under capacitating conditions at 1 h. We then assigned this fluorescence intensity a value of 0 by adjusting the settings such that no fluorescence was observed in BCECF-AM labelled oocytes in 0 mM procaine medium. All other oocytes incubated under 1, 2.5 and 5 mM procaine conditions were imaged with identical settings.

F-actin Distribution

The distribution of F-actin in horse oocytes was assessed as described previously by Van den Broeke et al. [39]. Oocytes were fixed for 30 min in 4% paraformaldehyde in DPBS at room temperature. After being washed twice in wash medium, the oocytes were permeabilized using 0.1% Triton X-100 in DPBS for 1 h at room temperature. Subsequently, oocytes were washed twice in wash medium and incubated with 40 µM FITC-labelled phalloidin in DPBS for 1 h at room temperature. Next, the oocytes were washed in DPBS and mounted on glass slides as described previously. The intensity of the FITC signal correlates with the amount of F-actin. In this study we considered the amount of F-actin in mature oocytes as the reference intensity. Increased or similar FITC intensity indicated the beginning of the cell cycle whereas a decreased FITC signal indicated the end of cell cycle associated with the preparation for cytokinesis.

Sperm Motility Assessment

To assess the combined effects of MitoTracker Green FM and DMSO on sperm motility, parameters of MitoTracker Green FM labelled sperm in suspension were evaluated using a computer-assisted sperm analyzer (CASA: Hamilton-Thorne motility analyzer Ceros version 12.3d; Hamilton-Thorne Research,

Beverly, MA, USA). Under defined capacitating conditions, BSA was replaced with PVA to avoid the marked sperm agglutination noted for stallion sperm after centrifugation in BSA-containing medium [12]. For each analysis, 10 µl of sperm solution diluted in non-capacitating medium was mounted on a pre-warmed glass slide (Marienfeld, Lauda-Königshofen, Germany) and maintained at 37°C using a minitherm stage warmer. Five randomly selected microscopic fields in the center of the slide were scanned 4 times each, generating 20 scans for every sample. The mean of the 5 scans for each sample was used for statistical analysis. The settings of the CASA-software HTR 12.3 for analyzing motility parameters of stallion sperm, were based on Loomis and Graham [40] and described previously by Hoogewijs et al. [41]. To evaluate the effect on sperm viability of 0, 200, 400, 800 and 1000 nM MitoTracker Green FM dissolved respectively in 0, 0.025, 0.05, 0.10 and 0.125% DMSO, the percentages of motile and progressively motile sperm were assessed. To assess the effect of 0, 1, 2.5 and 5 mM procaine on hypermotility parameters of sperm pre-labelled with 200 nM MitoTracker Green FM in 0.025% DMSO or non-labelled sperm, 2 motility parameters were evaluated: amplitude of lateral head displacement (ALH, in µm; ALH is the mean width of head oscillations), curvilinear velocity (VCL, in µm/s; VCL is the average velocity of a sperm head along its actual, two-dimensional curvilinear trajectory). Finally, an increase in these 2 motility parameters, ALH and VCL, was used to demonstrate hyperactivated motility in stallion sperm [6, 12].

Microscopic Imaging

Embryonic development was assessed using a CCD ICD-46E camera (Ikegami Tsushinki Co. Ltd., Japan) attached to an Olympus IX70 inverted microscope (Olympus Belgium N.V., Aartselaar, Belgium). Images of cleaved oocytes were acquired using the Image Database program (Leica, Van Hopplynus N.V., Brussel, Belgium).

Sperm labelling by various MitoTracker Green FM concentrations, sperm penetration through the zona pellucida, second polar body formation and DNA configuration of embryo development stages, the cortical granule distribution, cytoplasmic pH and F-actin distribution were determined by means of fluorescence microscopy using a Leica DM 5500 B microscope equipped with excitation filters with band pass 340/380 nm, 450/490 nm, 560/40 nm and a 120 W mercury lamp. MitoTracker Green FM, Hoechst 33342, LCA-FITC, BCECF-AM and phalloidin-FITC were excited using 490 nm, 345 nm, 495 nm, 490 nm and 495 nm wavelengths, respectively. The emission spectra were detected by Blue (BP 470/40 nm) and Green (LP 515 nm) filters corresponding to the emission peaks of the dyes at respectively 516 nm, 478 nm, 519 nm, 530 nm and 519 nm. Images were acquired using the Image Database program (Leica, Van Hopplynus N.V., Brussel, Belgium). The various fluorophores were checked for signal overlap; no bleed through of signals was detected.

Sperm penetration through the zona pellucida, DNA configuration, the cortical granule and F-actin distribution were confirmed by confocal microscopy using a Leica TCS SPE-II laser scanning spectral confocal system (Leica Microsystems GmbH; Wetzlar, Germany), equipped with an ACS APO 63X oil immersion objective (Leica) and linked to a DM 2500 upright microscope (Leica Microsystems). The fluorescent dyes were excited using a diode laser and analyzed using similar detection filters to those described for fluorescence microscopy. The images were obtained using Leica confocal software. For each wavelength, digital optical sections were collected using Z-series acquisition every 0.5 µm. Corresponding DIC images and images of lacmoid-stained oocytes were acquired using the Leica DM 5500 B fluorescence microscope described above.

Oocyte cleavage, second polar body formation and DNA configuration were confirmed by confocal microscopy using an inverted Nikon A1R confocal microscope (Nikon Instruments, Paris, France), mounted on a Nikon Ti body, using a 60×/1.4 Plan Apo oil immersion lens. Hoechst was excited using a 405 nm diode laser and a 488 nm Argon laser was used for simultaneous DIC imaging. Images were acquired using Nikon Elements Software and a pinhole setting of 1 Airy unit and constant acquisition

settings (laser power, gain and offset, scan speed). Digital optical sections were collected across an axial range that spanned the oocyte, at a step size of 1 μm.

Statistical Analysis

The effect of the combination of MitoTracker Green FM and DMSO on sperm motility parameters, the effect of different concentrations of procaine on embryonic development, the relative cytoplasmic pH change induced by different concentrations of procaine and the amount of F-actin in the cortical region were assessed by analysis of variance (ANOVA). Significant differences were determined using repeated measures ANOVA with Greenhouse-Geisser and Bonferroni correction, as implemented in the general linear model. Scheffé post-hoc tests were performed for pairwise comparisons. Differences were considered significant if $P<0.05$.

The effect of different fertilization conditions on sperm-oocyte penetration and the effect of procaine on cortical granule reaction induction were analyzed by binary logistic regression for binomially distributed data. Where differences existed, further comparisons of groups were performed by chi-square analysis (χ^2 fit tests). All experiments were repeated three times. Differences were considered significant if $P<0.05$. All analyses were performed using SPSS version 20 for Windows (SPSS IBM, Brussels, Belgium).

RESULTS

Effect of Procaine and MitoTracker Green FM on Sperm Motility Characteristics

To assess the effect of MitoTracker Green FM and DMSO on sperm motility, 10 ml sperm suspensions (100×10^6 spermatozoa/ml) were incubated for 30 min with various concentrations of this mitochondrion specific stain dissolved in DMSO. In the control sperm suspension (0 nM MitoTracker Green FM, 0 % DMSO) in our study, 82 ± 3 % of the spermatozoa were motile and 57 ± 4 % were progressively motile. Incubation with 200 nM MitoTracker Green FM and 0.025 % DMSO did not significantly affect motility (total motility: 78 ± 3 %; P = 0.32, progressive motility: 61 ± 2 %; P = 0.21). However, incubation with 0.05 % DMSO, irrespective of the additional presence of 400 nM MitoTracker Green FM, depressed motility (P = 0.01 and 0.03 for total and progressive motility, respectively). Total (69 ± 4 %) and progressive motility (47 ± 5 %) in the presence of 400 nM MitoTracker Green FM (Figure 1A) and total (71 ± 2 %) and progressive motility (42 ± 3 %) in the presence of 0.05% DMSO without MitoTracker did not differ (P = 0.31 and 0.15 for total and progressive motility, respectively). Higher concentrations of DMSO further disrupted both total and progressive sperm motility independent of the inclusion of MitoTracker Green FM, although the latter appeared to have an additional inhibitory effect on total but not progressive motility (Figures 1A and B). We note that the presence of 0.1 % DMSO also resulted in abnormal sperm movement. We concluded that 200 nM MitoTracker Green FM was the most suitable concentration for assessing sperm penetration through the zona pellucida, since there was no observable effect on gross sperm motility while a clear MitoTracker Green FM signal could be observed in the sperm mid-piece (Figure 1B). The DMSO and MitoTracker Green FM concentrations used were relatively low compared to those used in successful *in vitro* fertilization experiments with bovine [42] and mouse [43] gametes.

To assess the effect of the various procaine, MitoTracker Green FM and DMSO concentrations on sperm hypermotility, non-labelled and Mitotracker Green FM labelled (200 nM MitoTracker Green FM in 0.025% DMSO) sperm preparations (10×10^6 spermatozoa/ml) were first incubated for 6 h in capacitating conditions with an elevated pH (7.9) and subsequently for 30 min in various procaine concentrations (0, 1, 2.5 and 5 mM). Compared to procaine-free capacitating conditions (ALH: 4.0 ± 0.3 μm and VCL: 110 ± 3 μm/s), sperm ALH and VCL measurements were significantly higher when procaine was included (1 mM: ALH 5.9 ± 0.4 μm and VCL 147 ± 6 μm/s; 2.5 mM: ALH 7.1 ± 0.3 μm and VCL 185 ± 8 μm/s and 5 mM: ALH 7.0 ± 0.2 μm and VCL 187 ± 13 μm/s) and became more pronounced as the procaine

concentration increased. In accordance with the motility data described above, no significant effect on sperm hypermotility parameters was observed when sperm suspensions were pre-labelled with 200 nM MitoTracker Green FM dissolved in 0.025% DMSO (0 mM: ALH 4.1 ± 0.2 μm and VCL 118 ± 6 μm/s; 1 mM: ALH, 5.7 ± 0.3 μm and VCL 153 ± 5 μm/s; 2.5 mM: ALH 7.2 ± 0.5 μm and VCL 183 ± 6 μm/s and 5 mM: ALH 7.2 ± 0.3 μm and VCL 188 ± 11 μm/s) (Figure 2A and 2B).

Effect of Procaine and MitoTracker Green FM on Sperm Tail-Associated Protein Tyrosine Phosphorylation

To assess the effect of MitoTracker Green FM dissolved in DMSO and procaine on tail-associated protein tyrosine phosphorylation, sperm suspensions (10 x 10^6 spermatozoa/ml) were incubated for 6 h in 0, 1, 2.5 and 5 mM procaine at 2 different pHs, namely pH 7.4 (5% CO_2 in air incubation) and pH 7.9 (air incubation). Similar to previous reports [36, 44, 45], in these capacitating conditions tail-associated protein tyrosine phosphorylation was induced by an atmospheric air-related pH increase to 7.9, whereas procaine had no significant effect on this capacitation-associated event (pH 7.4 conditions: 0 mM, 11 ± 3%; 1 mM, 10 ± 2%; 2.5 mM, 10 ± 2% and 5 mM, 10 ± 3% compared to pH 7.9 conditions: 0 mM, 76 ± 2%; 1 mM, 75 ± 5%; 2.5 mM, 75 ± 3% and 5 mM, 72 ± 3%). Moreover, no effect of MitoTracker Green FM dissolved in DMSO was evident for rates of tail-associated protein tyrosine phosphorylation (pH 7.4 conditions: 0 mM, 10 ± 2%; 1 mM, 9 ± 2%; 2.5 mM, 11 ± 1% and 5 mM, 9 ± 2% compared to pH 7.9 conditions: 0 mM, 75 ± 5%; 1 mM, 74 ± 3%; 2.5 mM, 73 ± 5% and 5 mM, 70 ± 4%) (Figure 2C).

Procaine Does Not Induce Penetration of Equine Oocytes by Sperm In Vitro

In previous equine studies, fertilization after conventional IVF was assessed by determining the presence of at least 2 pronuclei in oocytes fixed 24 h after the *in vitro* fertilization incubation [8, 46, 47]. McPartlin et al. [6] assessed pronuclear formation and cleavage after 18 h of gamete co-incubation and an additional 24 h culture. This would not however differentiate definitively between true fertilization following sperm penetration, parthenogenetic activation of an unfertilized oocyte and oocyte cytokinesis. McPartlin et al. [6] did not report the oocyte-activation specific appearance of a second polar body in *in vitro* fertilized oocytes. We consider definitive proof of fertilization to include the presence of at least one sperm in the cytoplasm of the oocyte as assessed using; (1) labelled spermatozoa e.g. with 200 nM MitoTracker Green FM shortly before gamete co-incubation to label the mitochondria in the mid-piece [42] or; (2) post-fixation lacmoid staining of *in vitro* fertilized oocytes. In addition, the formation of the second polar body could be assessed by both Hoechst staining and light microscopic evaluation (3) and would confirm completion of the second meiotic division. Equine gamete co-incubation in the presence of 0, 1, 2.5 or 5 mM procaine (Figure 3a) did not result in sperm penetration through the zona pellucida in any cases (0 ± 0%) as assessed by MitoTracker Green FM pre-labelling. Neither did the presence of cumulus cells around the oocytes affect sperm-oocyte penetration rates. Oocytes activated parthenogenetically using ionomycin (Figure 3b) were used as a negative control, and also showed no evidence of MitoTracker Green FM labelling in the oocyte cytoplasm. As a positive control for stability of the stain, sperm were injected into mature (MII) equine oocytes by ICSI (Figure 3c); in these oocytes the sperm tail was clearly visible inside the oocyte cytoplasm (P-value < 0.001 for all comparisons). The failure of oocyte penetration during IVF was confirmed using unlabelled sperm and post-fixation lacmoid staining (Figure 3d, 3e and 3f). Furthermore, none of the procaine treated oocytes formed a second polar body as evidence of completion of the second meiotic division (0 ± 0%). By contrast, 89 ± 7% of ICSI fertilized oocytes showed a normal second polar body containing condensed DNA (see Figure 3c'). Together these data support the hypothesis that procaine does not support sperm penetration or *in vitro* fertilization but instead triggers fertilization-independent cytoplasmic cleavage.

Procaine Induces Cell Cleavage up to the 8-16 Cell Stage

After 2.5 days of culture, we observed a degenerative effect of 5 mM procaine on the oocyte. In capacitating conditions, 7 ± 3% of completely cumulus-denuded oocytes (CD) and 5 ± 5% of partially cumulus-denuded oocytes (PD) degenerated; in 1 mM procaine 8 ± 4% CD and 7 ± 4% PD degenerated;

in 2.5 mM procaine 12 ± 3% CD and 10 ± 3% PD; and in 5 mM procaine 38 ± 6% CD and 27 ± 4% PD degenerated. This suggested a concentration-dependent toxic effect of procaine on developing embryos that could be partially inhibited by the presence of cumulus cells around the oocytes during the 24 h gamete co-incubation ($P < 0.001$ for all comparisons; Figure 4). Interestingly, in our hands in the presence of 2.5 mM procaine, 44 ± 12% CD and 56 ± 4% PD oocytes cleaved, whereas cleavage was significantly reduced in the presence of 5 mM procaine (12 ± 6% CD and 8 ± 4% PD). Significantly more oocytes started to cleave when the cumulus investment was left in place during gamete co-incubation ($P < 0.001$ for all comparisons; Figure 4 and 5). A significantly higher cleavage rate was achieved in ICSI-fertilized oocytes (78 ± 6% of injected oocytes; $P < 0.001$). Tellingly, oocytes that cleaved in the presence of procaine never developed beyond the 8-16 cell stage even though, after exposure to 2.5 mM procaine in capacitating conditions, 70 ± 5% CD and 67 ± 8% PD cleaved oocytes reached the 8-16 cell stage (31 ± 2% CD and 37 ± 4% PD incubated oocytes). A similar pattern was observed after exposure to 5 mM procaine, when 63 ± 3% CD and 65 ± 5% PD cleaved oocytes developed to the 8-16 cell stage (8 ± 2% of CD and 5 ± 1% of PD incubated oocytes). The presence of cumulus cells around the oocyte did not have a significant effect on the percentage of cleaved oocytes that reached the 8-16 cell stage ($P > 0.14$ for all comparisons). In short, cleaved embryos that formed in the presence of procaine never (0 ± 0%) reached the blastocyst stage whereas 15 ± 6% of ICSI oocytes did develop to blastocysts (Figure 5). After 5-6 days of incubation, all presumptive embryos derived from procaine treatments started to degenerate. Moreover, none of these parameters differed significantly between oocytes incubated in the presence or absence of spermatozoa, indicating that procaine-induced oocyte cytokinesis was sperm-independent (Figure 4 and 5).

Procaine-Induced Embryonic Cleavage Is Associated with Aberrant DNA Segregation and Fragmentation

As indicated above, procaine triggered cleavage of horse oocytes. We also analyzed the effect of procaine (0, 1, 2.5 and 5 mM procaine in capacitating conditions) on nuclear configuration during embryo development. After 24 h incubation in the presence of 5 mM procaine, we observed significantly more DNA fragmentation in the oocytes than in oocytes exposed to 0, 1, or 2.5 mM procaine. Moreover, the incidence of oocytes with fragmented DNA was higher for the completely denuded (CD) than for the partially cumulus-denuded oocytes (PD) (Figure 6). In addition, in 0 (control) and 1 mM procaine, the majority of oocytes displayed a normal metaphase spindle (MI: 32 ± 3 and MII: 55 ± 9%) indicating that procaine up to 1 mM did not affect the DNA configuration (Figure 6). By contrast, after exposure to 2.5 or 5 mM procaine one (1F) or two (2F) very condensed fragments of DNA were observed instead (2.5 mM procaine: 32 ± 3% 1F and 57 ± 3% 2F; 5 mM procaine: 20 ± 5% 1F and 50 ± 10% 2F, respectively; Figure 6). The presence of cumulus cells around the oocytes during procaine exposure ($P < 0.001$ for all comparisons) protected against DNA fragmentation. The formation of normal healthy (pro)nuclei (1 or 2 PN), indicating that oocytes had undergone fertilization or viable parthenogenesis, was a rare finding in procaine-treated oocytes (less than 3 ± 3%; Figure 6). In contrast to oocytes incubated with sperm at various procaine concentrations, 87 ± 5% of ICSI fertilized oocytes formed 2 pronuclei 24 h after injection, using the same maturation and culture conditions used for procaine-exposed oocytes ($p<0.001$ for all comparisons).

During development of embryos formed in the presence of procaine, the majority of the apparent daughter cells did not contain DNA at all, while others displayed condensed, fragmented pieces of DNA (Figure 7). In ICSI-fertilized oocytes, every cell contained a nucleus (Figure 7). None of these parameters evaluated after procaine exposure differed between oocytes incubated in the presence or absence of spermatozoa, again indicating that procaine-induced cleavage events were sperm-independent ($P > 0.11$ for all comparisons; Figure 6 and 7).

Procaine Does Not Induce Cytoplasmic Calcium Oscillations in Horse Oocytes

With respect to what has been reported for various mammalian species [38, 48, 49], we wanted to determine whether procaine-induced horse oocyte activation evoked calcium oscillations. To this end, we ratiometrically measured calcium oscillations in procaine- and ionomycin-exposed, and in ICSI-fertilized, horse oocytes. In the case of ICSI, fertilized oocytes exhibited a series of cytoplasmic calcium rises over at least 16 h (Figure 8c). This pattern was similar to that reported previously in mouse [48], human [38, 48] and equine [50] oocytes. Similar to reports for mouse and human oocytes [51, 52], parthenogenetic activation by ionomycin induced a single early rise in intracellular calcium (Figure 8b). By contrast, incubation of *in vitro* matured equine oocytes in 2.5 mM procaine did not trigger cytoplasmic calcium fluctuations during a 6 h incubation (Figure 8a).

Procaine Does Not Induce Cortical Granule Exocytosis

To alternatively assess calcium signaling during oocyte activation we used lectin staining (LCA-FITC) to determine whether procaine could induce the cortical reaction. After oocyte maturation, we found that the cortical granules were concentrated in the periphery of the cytoplasm of most oocytes (83 ± 3%; Figure 9a). When the oocytes were subsequently incubated for 6 h in capacitating conditions (0% procaine), the same cortical granule pattern was generally maintained (85 ± 5%; Figure 9d). Ionomycin-activated and ICSI fertilized oocytes lost their cortical granules, indicating that the oocytes had undergone calcium-dependent cortical granule extrusion (ionomycin: 85 ± 4%, ICSI: 82 ± 7%; Figure 9b and 9c). By contrast, procaine-activated oocytes did not extrude their cortical granules during a 6 h procaine/IVF incubation; instead a proportion of the cortical granules were maintained in the periphery of the cytoplasm and even more were redistributed to more centrally in the cytoplasm (2.5 mM procaine: 76 ± 7%; 5 mM procaine: 68 ± 5%; Figure 9e and 9f).

Procaine Induces Cytoplasmic Alkalinization in Horse Oocytes

Using BCECF-AM staining, we ratiometrically assessed the effect on horse oocytes of exposure to 0, 1, 2.5, 5 and 10 mM procaine. It transpired that procaine induced a rapid, concentration-dependent increase in the BCECF-AM ratio during the first hour of incubation (after 1 h in 0 mM procaine: 1.13 ± 0.06; in 1 mM procaine: 1.33 ± 0.06; in 2.5 mM procaine: 1.87 ± 0.10; in 5 mM procaine: 2.97 ± 0.15; and in 10 mM procaine: 5.13 ± 0.21) which remained constant during the remainder of the 6 h culture period ($P > 0.11$ for all comparisons; Figure 10a). The procaine concentration dependent increase in BCECF-AM fluorescence in horse oocytes at 1 h of incubation is shown in Figure 10b. The BCECF-AM fluorescence in horse oocytes incubated in 0 mM procaine was assigned as the baseline to which oocytes exposed to procaine differed significantly ($p<0.001$).

Procaine Induces Depolymerization of Cortical F-actin in Horse Oocytes

To assess the effect of procaine on cortical F-actin turnover in preparation for cytokinesis, we used phalloidin-FITC staining. Two different phalloidin-FITC staining patterns were observed (Figure 11). The amount of F-actin present in the cortical region of mature oocytes was relatively high (Figure 11a). After 18 h exposure to procaine (2.5 mM), the majority of oocytes showed a clear decrease in F-actin abundance (Figure 11d; only 24 ± 6% oocytes retained the more intense phalloidin labelling pattern), whereas in standard conditions (0 mM procaine) the F-actin pattern was similar to that seen in pre-incubation MII oocytes (81 ± 5%; Figure 11c; $P<0.001$). As expected, 18 h after injection ICSI-fertilized oocytes also showed a decrease in F-actin abundance (Figure 11b) with only 26 ± 5% retaining the abundant phalloidin labelling pattern. The similarity in actin cytoskeleton depolymerization in ICSI-fertilized and procaine-treated oocytes indicates that at least some aspects of procaine-induced cytokinesis of equine oocytes are similar to fertilization-induced cleavage.

DISCUSSION

The principal aim of this study was to determine how procaine-induced hyperactivation of protein tyrosine phosphorylated stallion spermatozoa allows the latter to fertilize mature equine oocytes *in vitro*. Instead, we found that procaine had a direct effect on equine oocytes, inducing cytokinesis followed by further cleavage divisions up to the 8-16 cell stage, which was not accompanied by sperm penetration or second polar body formation. Interestingly, we also noted that in procaine-activated oocytes the DNA in the metaphase II plate condensed without prior formation of a proper pronucleus. During cytoplasmic cleavage, these condensed DNA fragments segregated to one of the two daughter cells only, indicating that DNA duplication did not take place. Moreover, we clearly demonstrated that procaine-induced cytokinesis in equine oocytes was not stimulated by a rise in cytoplasmic calcium, in marked contrast to the situation in oocytes fertilized by ICSI or parthenogenetically-activated by ionomycin. Instead, exposure of equine oocytes to procaine induced a rapid increase in cytoplasmic pH followed by a pH–dependent reduction in F-actin, both of which are important steps in cytokinesis [29].

The first important observation was that tail-associated protein tyrosine phosphorylated, hyperactivated stallion spermatozoa were not able to penetrate equine oocytes *in vitro* despite the presence of 0, 1, 2.5 or 5 mM procaine, as evidenced by incubating oocytes with spermatozoa labelled with MitoTracker Green FM. These results were confirmed on oocytes treated with unlabelled sperm using post-fixation lacmoid staining. That similar cleavage rates were achieved irrespective of the presence of spermatozoa, further suggests that the primary effect of procaine was not to trigger sperm penetration. Moreover, oocytes that cleaved in the presence of procaine did not form a second polar body, suggesting failure of normal oocyte activation. By contrast, the injection of a single sperm cell into an oocyte by ICSI was followed by (1) normal second polar body formation and (2) normal pronucleus formation, demonstrating that the incubation conditions were adequate for oocyte maturation and embryo development. Possibly, an oviduct derived factor is essential for equine oocyte penetration by a sperm, but we do not yet know whether that factor is implicated in modifying the cumulus/zona pellucida or the sperm surface. Without that oviduct factor, it appears that sperm cannot fertilize the oocyte, regardless of the presence of cumulus cells.

In a number of previous studies, the success of fertilization was determined exclusively by the presence of 2 pronuclei at 20-24 h after sperm-oocyte co-incubation [6, 8, 46]. Although we agree that the detection of two pronuclei and cell cleavage are generally indicative of fertilization in the horse, neither parthenogenetic activation followed by the formation of two maternal pronuclei nor oocyte cytokinesis can be excluded by these end-points. That is why we decided to determine whether a sperm cell could be shown to enter the oocyte under the procaine/capacitating conditions. Labelling bull spermatozoa with MitoTracker Green FM had previously been shown not to interfere with fertilization and embryo development in a bovine IVF system [42]. Because horse-specific fertilization characteristics are not yet known, and to exclude any possible interfering effect of MitoTracker Green FM and DMSO on sperm-oocyte penetration, unlabelled sperm and post-fixation lacmoid staining were used to confirm the failure of sperm penetration. Moreover, pre-labelling sperm with MitoTracker Green FM dissolved in DMSO did not affect sperm (hyper)motility or tail-associated protein tyrosine phosphorylation. Thus, MitoTracker Green FM sperm pre-labelling was not responsible for failure of sperm-oocyte penetration in procaine/capacitating conditions and pre-labelling sperm with this dye may be a valuable additional tool for assessing fertilization in the horse, as has been shown in other mammalian species [42, 43]. In our study, not a single spermatozoon was observed in the cytoplasm of an oocyte in any of the IVF conditions, and we conclude that fertilization does not occur under normal or procaine-supplemented capacitating conditions. We also note that, while procaine induced cleavage of the oocytes, none of the resulting ‘embryos’ formed a visible second polar body. Previous studies have not addressed the presence of a second polar body in the cleaved oocytes [6, 8]. The absence of the second polar body is a clear indication that the second meiotic division of the maternal DNA is not completed normally. In this respect, DNA fragmentation is also visible in both nuclei of the two-cell stage procaine-induced embryo depicted by McPartlin et al. [6]. We speculate that the aberrant chromatin condensation and fragmentation

in procaine-treated oocytes prevents development beyond the third or fourth cytoplasmic cleavage. By contrast, sperm injected oocytes developed into normal blastocysts and showed normal second polar body formation, normal pronucleus formation, and had no signs of unequal DNA division or DNA condensation and fragmentation, demonstrating that both the oocytes and embryo culture conditions were adequate to support embryo development.

A second important observation was that procaine induced a rise in cytoplasmic pH in horse oocytes. At concentrations of ≥ 5 mM procaine, the resulting high pH exerted a degenerative effect on the oocytes that was not observed at ≤ 2.5 mM. In sea urchin eggs, procaine acts as a proton acceptor and thereby mediates cytoplasmic alkalinization [28]. At 5 mM procaine, the rise in cytoplasmic pH was presumably too high and therefore induced oocyte degeneration. This effect could be partially countered by the presence of a cumulus cell investment around the mature oocyte. At lower concentrations of procaine (2.5 mM), the rise in cytoplasmic pH did not induce degeneration but instead triggered cytoplasmic cleavage up to the 8-16 cell stage. This procaine concentration most likely induced the appropriate rise in cytoplasmic pH to activate equine oocytes, whereas a lower procaine concentration did not provoke sufficient cytoplasmic pH change to activate cytokinesis. Similar to our results, exposure of sea urchin eggs to procaine induced a cytoplasmic pH increase [53]. Procaine, and some other local anesthetics, are tertiary amines that show characteristics of weak bases. Winkler and Grainger [28] demonstrated that procaine acted as a proton acceptor within the oocyte cytoplasm. In sea urchin eggs, elevated cytoplasmic pH mediated cortical non-filamentous actin polymerization and a rapid increase in the amount of F-actin [29, 54]. Elevated pH acts directly on actin/actin binding protein complexes [55, 56]. The polymerization of cortical non-filamentous actin to F-actin, to construct a functional contractile ring to mediate cell cleavage, followed by a decrease in F-actin is required for cytoskeleton reorganization prior to cytokinesis [54, 57, 58].

It therefore appears that procaine can induce cytokinesis in equine oocytes, but that this is not accompanied by normal nuclear division and mitosis. As mentioned above, after 18 h incubation in 2.5 mM procaine, the DNA configuration changed from a metaphase II plate to one or two very condensed DNA fragments, without prior pronucleus formation. Moreover, when cytoplasmic cleavage was initiated, the DNA did not divide appropriately, such that during the subsequent oocyte divisions the majority of the ‘cells’ did not contain nuclear material. An additional explanation can be found in studies in other systems; in cultured myogenic cells, procaine exerts a concentration dependent toxic effect on the DNA [59] and, in fertilized sea urchin eggs, high concentrations of procaine (10 mM) were associated with the inhibition of DNA synthesis and the polymerization of tubulin, which has an important function in the construction of the meiotic spindle [60, 61]. These events appear to be related to the procaine-induced elevation in cytoplasmic pH [61] and are most probably the cause of the DNA fragmentation that we observed. It is also unlikely that this compacted DNA could initiate embryonic genome activation, such that more advanced stages would inevitably degenerate. In conclusion, we assume that 2.5 mM procaine induced the appropriate cytoplasmic pH shift to cause cytokinesis without DNA replication.

A third important observation was that procaine did not induce oocyte activation via the normal pathway, which begins with a rise in cytoplasmic calcium. In various mammalian species, oocyte activation is induced by a cytoplasmic calcium rise soon after fertilization or after contact with the parthenogenetic agent [62]. In our study we found that, as reported for other mammalian species, ionomycin induced an early single cytoplasmic calcium rise, whereas ICSI induced calcium oscillations, in mature oocytes. A rise in oocyte cytoplasmic calcium is generally accepted to induce both ‘early’ and ‘late’ events of the fertilization process, where the early events include the cortical reaction, sodium influx and a respiratory burst, and the late events include an increase in intracellular pH, DNA and protein synthesis and chromosome replication and segregation [63, 64]. However, after 6 h exposure to 2.5 mM procaine no cytoplasmic calcium rise was observed in equine oocytes and neither did procaine induce the calcium dependent cortical reaction. Similar observations have been reported in sea urchin eggs [65, 66] in which

procaine failed to trigger either calcium influx [65] or release from intracellular calcium stores [66]. Also in pig [21, 22] and cattle [23, 24], the oocyte- activation associated calcium rise could be inhibited by injecting procaine into the cytoplasm, because even low concentrations (max 200 μM) of procaine were able to block the ryanodine receptors on the calcium channels of the cytoplasmic calcium stores. These observations reinforce the conclusion that calcium oscillations early in fertilization and the subsequent cortical reaction, as seen in horse oocytes subjected to ICSI, do not take place in the presence of procaine.

Finally, we showed that the total amount of F-actin in the equine oocyte decreased significantly during 18 h of incubation in the presence of 2.5 mM procaine in a similar fashion to that observed in sperm injected oocytes. Reduction in F-actin has to occur at the end of the cell cycle in preparation for cytokinesis [30]. Moreover, a cyclic increase and decrease in the amount of cortical F-actin has been observed during early cleavage divisions, with a peak near the beginning of the cell cycle and a trough during cytokinesis [30]. In sea urchin eggs, weak bases such as procaine can stimulate pH mediated actin turnover [67-70]. Moreover, ADF/cofilin (AC) proteins exhibit a pH dependent role in F-actin turnover [71, 72] consisting of an alkalinity-associated increase in F-actin depolymerization activity, with a critical concentration around neutral pH [73], and a temporary concentration at the contractile ring during cytokinesis [74]. ADF/cofilin (AC) proteins have been found in all eukaryotic cells thus far examined [75-78] and are therefore likely to be involved in cytokinesis of the horse zygote or oocyte.

It may be argued that sea urchins are not representative of fertilization events in mammals. However, similarities in fertilization-mediated events, like calcium induced oocyte activation and the subsequent cortical reaction, have been reported [79]. Following the cytoplasmic calcium transient, an efflux of protons from the egg results in an elevated cytoplasmic pH in fertilized sea urchin eggs [80], which initiates cortical F-actin turnover [29, 30]. However, the physiological role of a raised cytoplasmic pH in mammalian oocyte activation is not clear [62]. Further research is required to elucidate whether such events are evolutionarily conserved between the sea urchin and mammalian species. More importantly, proof is required that a rise in cytoplasmic pH contributes to oocyte activation during normal fertilization or ionomycin treatment in horses. Theoretically, a pH rise in a horse oocyte could induce: 1) a non-physiological activation of pH-sensitive enzymes involved in actin polymerization / cytokinesis or, as in sea urchins, 2) a physiological response that results in cytokinesis.

In conclusion, we have shown that procaine does not facilitate penetration of horse oocytes by spermatozoa, despite directly stimulating hyperactivated motility in stallion spermatozoa. In our hands, procaine instead induced a pH rise dependent cytokinesis in equine oocytes, without inducing an intracellular calcium increase, albeit only over a small range of procaine concentrations. Cleaved oocytes developed to the 8-16 cell stage without undergoing proper DNA duplication and without the formation of a second polar body. Moreover, the unequally divided DNA deteriorated by becoming condensed and fragmented.

ACKNOWLEDGMENT

The authors wish to thank Petra Van Damme and Isabel Lemahieu for their excellent technical assistance. Fresh stallion semen was kindly provided by the Clinic of Reproduction and Obstetrics of Large Animals, Merelbeke, Belgium.

REFERENCES

1. Palmer E, Bezard J, Magistrini M, Duchamp G. In vitro fertilization in the horse. A retrospective study. J Reprod Fertil Suppl 1991; 44:375-384.
2. Bézard J, Magistrini M, Battut I, Duchamp G, Palmer E. In vitro Fertilization in the Mare. Recueil De Medecine Veterinaire 1992; 168:993-1003.
3. Dell'Aquila ME, Cho YS, Minoia P, Traina V, Fusco S, Lacalandra GM, Maritato F. Intracytoplasmic sperm injection (ICSI) versus conventional IVF on abottoir-derived and in vitro-matured equine oocytes. Theriogenology 1997; 47:1139-1156.
4. Dell'Aquila ME, Cho YS, Minoia P, Traina V, Lacalandra GM, Maritato F. Effects of follicular fluid supplementation of in-vitro maturation medium on the fertilization and development of equine oocytes after in-vitro fertilization or intracytoplasmic sperm injection. Human Reproduction 1997; 12:2766-2772.
5. Hinrichs K, Loux SC. Hyperactivated Sperm Motility: Are Equine Sperm Different? Journal of Equine Veterinary Science 2012; 32:441-444.
6. McPartlin LA, Suarez SS, Czaya CA, Hinrichs K, Bedford-Guaus SJ. Hyperactivation of Stallion Sperm Is Required for Successful In Vitro Fertilization of Equine Oocytes. Biology of Reproduction 2009; 81:199-206.
7. McPartlin LA, Littell J, Mark E, Nelson JL, Travis AJ, Bedford-Guaus SJ. A defined medium supports changes consistent with capacitation in stallion sperm, as evidenced by increases in protein tyrosine phosphorylation and high rates of acrosomal exocytosis. Theriogenology 2008; 69:639-650.
8. Ambruosi B, Accogli G, Douet C, Canepa S, Pascal G, Monget P, Moros Nicolas C, Holmskov U, Mollenhauer J, Robbe-Masselot C, Vidal O, Desantis S, et al. Deleted in malignant brain tumor 1 is secreted in the oviduct and involved in the mechanism of fertilization in equine and porcine species. Reproduction 2013; 146:119-133.
9. Cahalan MD. Local anesthetic block of sodium channels in normal and pronase-treated squid giant axons. Biophys J 1978; 23:285-311.
10. Mujica A, Neri-Bazan L, Tash JS, Uribe S. Mechanism for procaine-mediated hyperactivated motility in guinea pig spermatozoa. Mol Reprod Dev 1994; 38:285-292.
11. Ortgies F, Klewitz J, Gorgens A, Martinsson G, Sieme H. Effect of procaine, pentoxifylline and trolox on capacitation and hyperactivation of stallion spermatozoa. Andrologia 2012; 44 Suppl 1:130-138.
12. Loux SC, Crawford KR, Ing NH, Gonzalez-Fernandez L, Macias-Garcia B, Love CC, Varner DD, Velez IC, Choi YH, Hinrichs K. CatSper and the relationship of hyperactivated motility to intracellular calcium and pH kinetics in equine sperm. Biol Reprod 2013; 89:123.
13. Kirichok Y, Navarro B, Clapham DE. Whole-cell patch-clamp measurements of spermatozoa reveal an alkaline-activated Ca2+ channel. Nature 2006; 439:737-740.
14. Quill TA, Sugden SA, Rossi KL, Doolittle LK, Hammer RE, Garbers DL. Hyperactivated sperm motility driven by CatSper2 is required for fertilization. Proc Natl Acad Sci U S A 2003; 100:14869-14874.
15. Qi H, Moran MM, Navarro B, Chong JA, Krapivinsky G, Krapivinsky L, Kirichok Y, Ramsey IS, Quill TA, Clapham DE. All four CatSper ion channel proteins are required for male fertility and sperm cell hyperactivated motility. Proc Natl Acad Sci U S A 2007; 104:1219-1223.
16. Nakanishi T, Ishibashi N, Kubota H, Inoue K, Ogonuki N, Ogura A, Kashiwabara S, Baba T. Birth of normal offspring from mouse eggs activated by a phospholipase Czeta protein lacking three EF-hand domains. J Reprod Dev 2008; 54:244-249.
17. Kashir J, Heindryckx B, Jones C, De Sutter P, Parrington J, Coward K. Oocyte activation, phospholipase C zeta and human infertility. Hum Reprod Update 2010; 16:690-703.
18. Versieren K, Heindryckx B, Lierman S, Gerris J, De Sutter P. Developmental competence of parthenogenetic mouse and human embryos after chemical or electrical activation. Reprod Biomed Online 2010; 21:769-775.
19. Kim JW, Kim SD, Yang SH, Yoon SH, Jung JH, Lim JH. Successful pregnancy after SrCl2 oocyte activation in couples with repeated low fertilization rates following calcium ionophore treatment. Syst Biol Reprod Med 2014; 60:177-182.
20. Carvacho I, Lee HC, Fissore RA, Clapham DE. TRPV3 channels mediate strontium-induced mouse-egg activation. Cell Rep 2013; 5:1375-1386.
21. Mattioli M, Barboni B, Gioia L, Loi P. Cold-induced calcium elevation triggers DNA fragmentation in immature pig oocytes. Mol Reprod Dev 2003; 65:289-297.
22. Petr J, Rajmon R, Lanska V, Sedmikova M, Jilek F. Nitric oxide-dependent activation of pig oocytes: role of calcium. Mol Cell Endocrinol 2005; 242:16-22.
23. Yue C, White KL, Reed WA, Bunch TD. The existence of inositol 1,4,5-trisphosphate and ryanodine receptors in mature bovine oocytes. Development 1995; 121:2645-2654.
24. Viets LN, Campbell KD, White KL. Pathways involved in RGD-mediated calcium transients in mature bovine oocytes. Cloning Stem Cells 2001; 3:105-113.
25. Carneiro GF, Liu IK, Hyde D, Anderson GB, Lorenzo PL, Ball BA. Quantification and distribution of equine oocyte cortical granules during meiotic maturation and after activation. Mol Reprod Dev 2002; 63:451-458.
26. Tsai PS, van Haeften T, Gadella BM. Preparation of the cortical reaction: maturation-dependent migration of SNARE proteins, clathrin, and complexin to the porcine oocyte's surface blocks membrane traffic until fertilization. Biol Reprod 2011; 84:327-335.

27. Saavedra MD, Mondejar I, Coy P, Betancourt M, Gonzalez-Marquez H, Jimenez-Movilla M, Aviles M, Romar R. Calreticulin from suboolemmal vesicles affects membrane regulation of polyspermy. Reproduction 2014; 147:369-378.
28. Winkler MM, Grainger JL. Mechanism of action of NH4Cl and other weak bases in the activation of sea urchin eggs. Nature 1978; 273:536-538.
29. Begg DA, Wong GK, Hoyle DH, Baltz JM. Stimulation of cortical actin polymerization in the sea urchin egg cortex by NH4Cl, procaine and urethane: elevation of cytoplasmic pH is not the common mechanism of action. Cell Motil Cytoskeleton 1996; 35:210-224.
30. Wong GK, Allen PG, Begg DA. Dynamics of filamentous actin organization in the sea urchin egg cortex during early cleavage divisions: implications for the mechanism of cytokinesis. Cell Motil Cytoskeleton 1997; 36:30-42.
31. Parrish JJ, Susko-Parrish J, Winer MA, First NL. Capacitation of bovine sperm by heparin. Biol Reprod 1988; 38:1171-1180.
32. Tremoleda JL, Stout TAE, Lagutina I, Lazzari G, Bevers MM, Colenbrander B, Galli C. Effects of in vitro production on horse embryo morphology, cytoskeletal characteristics, and blastocyst capsule formation. Biology of Reproduction 2003; 69:1895-1906.
33. Galli C, Colleoni S, Duchi R, Lagutina I, Lazzari G. Developmental competence of equine oocytes and embryos obtained by in vitro procedures ranging from in vitro maturation and ICSI to embryo culture, cryopreservation and somatic cell nuclear transfer. Animal Reproduction Science 2007; 98:39-55.
34. Heras S, Smits K, Leemans B, Van Soom A. Asymmetric histone 3 methylation pattern between paternal and maternal pronuclei in equine zygotes. Anal Biochem 2015; 471:67-69.
35. Smits K, Govaere J, Hoogewijs M, Piepers S, Van Soom A. A pilot comparison of laser-assisted vs piezo drill ICSI for the in vitro production of horse embryos. Reprod Domest Anim 2012; 47:e1-3.
36. Leemans B, Gadella BM, Sostaric E, Nelis H, Stout TA, Hoogewijs M, Van Soom A. Oviduct binding and elevated environmental ph induce protein tyrosine phosphorylation in stallion spermatozoa. Biol Reprod 2014; 91:13.
37. Martinez EA, Vazquez JM, Matas C, Gadea J, Alonso MI, Roca J. Oocyte penetration by fresh or stored diluted boar spermatozoa before and after in vitro capacitation treatments. Biol Reprod 1996; 55:134-140.
38. Nikiforaki D, Vanden Meerschaut F, Qian C, De Croo I, Lu Y, Deroo T, Van den Abbeel E, Heindryckx B, De Sutter P. Oocyte cryopreservation and in vitro culture affect calcium signalling during human fertilization. Hum Reprod 2014; 29:29-40.
39. Van den Broeke C, Radu M, Deruelle M, Nauwynck H, Hofmann C, Jaffer ZM, Chernoff J, Favoreel HW. Alphaherpesvirus US3-mediated reorganization of the actin cytoskeleton is mediated by group A p21-activated kinases. Proc Natl Acad Sci U S A 2009; 106:8707-8712.
40. Loomis PR, Graham JK. Commercial semen freezing: individual male variation in cryosurvival and the response of stallion sperm to customized freezing protocols. Anim Reprod Sci 2008; 105:119-128.
41. Hoogewijs M, Rijsselaere T, De Vliegher S, Vanhaesebrouck E, De Schauwer C, Govaere J, Thys M, Hoflack G, Van Soom A, de Kruif A. Influence of different centrifugation protocols on equine semen preservation. Theriogenology 2010; 74:118-126.
42. Sutovsky P, Navara CS, Schatten G. Fate of the sperm mitochondria, and the incorporation, conversion, and disassembly of the sperm tail structures during bovine fertilization. Biol Reprod 1996; 55:1195-1205.
43. Davies TJ, Gardner RL. The plane of first cleavage is not related to the distribution of sperm components in the mouse. Hum Reprod 2002; 17:2368-2379.
44. Gonzalez-Fernandez L, Macias-Garcia B, Velez IC, Varner DD, Hinrichs K. Calcium-calmodulin and pH regulate protein tyrosine phosphorylation in stallion sperm. Reproduction 2012; 144:411-422.
45. Aalberts M, Sostaric E, Wubbolts R, Wauben MW, Nolte-'t Hoen EN, Gadella BM, Stout TA, Stoorvogel W. Spermatozoa recruit prostasomes in response to capacitation induction. Biochim Biophys Acta 2013; 1834:2326-2335.
46. Hinrichs K, Love CC, Brinsko SP, Choi YH, Varner DD. In vitro fertilization of in vitro-matured equine oocytes: Effect of maturation medium, duration of maturation, and sperm calcium ionophore treatment, and comparison with rates of fertilization in vivo after oviductal transfer. Biology of Reproduction 2002; 67:256-262.
47. Mugnier S, Dell'Aquila ME, Pelaez J, Douet C, Ambruosi B, De Santis T, Lacalandra GM, Lebos C, Sizaret PY, Delaleu B, Monget P, Mermillod P, et al. New insights into the mechanisms of fertilization: comparison of the fertilization steps, composition, and structure of the zona pellucida between horses and pigs. Biol Reprod 2009; 81:856-870.
48. Vanden Meerschaut F, Nikiforaki D, Heindryckx B, De Sutter P. Assisted oocyte activation following ICSI fertilization failure. Reprod Biomed Online 2014; 28:560-571.
49. Kashir J, Deguchi R, Jones C, Coward K, Stricker SA. Comparative biology of sperm factors and fertilization-induced calcium signals across the animal kingdom. Mol Reprod Dev 2013; 80:787-815.
50. Bedford-Guaus SJ, Yoon SY, Fissore RA, Choi YH, Hinrichs K. Microinjection of mouse phospholipase C zeta complementary RNA into mare oocytes induces long-lasting intracellular calcium oscillations and embryonic development. Reprod Fertil Dev 2008; 20:875-883.
51. Swann K, Ozil JP. Dynamics of the calcium signal that triggers mammalian egg activation. Int Rev Cytol 1994; 152:183-222.
52. Tesarik J, Testart J. Treatment of sperm-injected human oocytes with Ca2+ ionophore supports the development of Ca2+ oscillations. Biol Reprod 1994; 51:385-391.

53. Shen SS, Steinhardt RA. Direct measurement of intracellular pH during metabolic derepression of the sea urchin egg. Nature 1978; 272:253-254.
54. Mabuchi I. Cleavage furrow: timing of emergence of contractile ring actin filaments and establishment of the contractile ring by filament bundling in sea urchin eggs. J Cell Sci 1994; 107 (Pt 7):1853-1862.
55. Tilney LG, Kiehart DP, Sardet C, Tilney M. Polymerization of actin. IV. Role of Ca++ and H+ in the assembly of actin and in membrane fusion in the acrosomal reaction of echinoderm sperm. J Cell Biol 1978; 77:536-550.
56. Tilney LG. Polymerization of actin. V. A new organelle, the actomere, that initates the assembly of actin filaments in Thyone sperm. J Cell Biol 1978; 77:551-564.
57. Mabuchi I. Effects of muscle proteins on the interaction between actin and an actin-depolymerizing protein from starfish oocytes. J Biochem 1982; 92:1439-1447.
58. Cline CA, Schatten G. Microfilaments during sea urchin fertilization: fluorescence detection with rhodaminyl phalloidin. Gamete Res 1986; 14:277-291.
59. Hagiwara Y, Ozawa E. Toxicity of local anaesthetics on myogenic cells in culture. J Pharmacobiodyn 1985; 8:106-113.
60. Coffe G, Foucault G, Raymond MN, Pudles J. Dual effect of procaine in sea urchin eggs. Inducer and inhibitor of microtubule assembly. Exp Cell Res 1985; 156:175-181.
61. Raymond MN, Foucault G, Coffe G, Pudles J. DNA synthesis and microtubule assembly-related events in fertilized Paracentrotus lividus eggs: reversible inhibition by 10 mM procaine. Eur J Cell Biol 1986; 40:296-302.
62. Jones KT. Mammalian egg activation: from Ca2+ spiking to cell cycle progression. Reproduction 2005; 130:813-823.
63. Epel D. The program of and mechanisms of fertilization in the echinoderm egg. American Zoologist 1975; 15:507-522.
64. De Petris S. Inhibition and reversal of capping by cytochalasin B, vinblastine and colchicine. Nature 1974; 250:54-56.
65. Zucker RS, Steinhardt RA, Winkler MM. Intracellular calcium release and the mechanisms of parthenogenetic activation of the sea urchin egg. Dev Biol 1978; 65:285-295.
66. Franks NP, Lieb WR. Molecular and cellular mechanisms of general anaesthesia. Nature 1994; 367:607-614.
67. Carron CP, Longo FJ. Relation of cytoplasmic alkalinization to microvillar elongation and microfilament formation in the sea urchin egg. Dev Biol 1982; 89:128-137.
68. Coffe G, Rola FH, Soyer MO, Pudles J. Parthenogenetic activation of sea urchin egg induces a cyclical variation of the cytoplasmic resistance to hexylene glycol-Triton X-100 treatment. Exp Cell Res 1982; 137:63-72.
69. Coffe G, Foucault G, Raymond MN, Pudles J. Tubulin dynamics during the cytoplasmic cohesiveness cycle in artificially activated sea urchin eggs. Exp Cell Res 1983; 149:409-418.
70. Moy GW, Brandriff B, Vacquier VD. Cytasters from sea urchin eggs parthenogenetically activated by procaine. J Cell Biol 1977; 73:788-793.
71. Lappalainen P, Drubin DG. Cofilin promotes rapid actin filament turnover in vivo. Nature 1997; 388:78-82.
72. Lappalainen P, Fedorov EV, Fedorov AA, Almo SC, Drubin DG. Essential functions and actin-binding surfaces of yeast cofilin revealed by systematic mutagenesis. Embo j 1997; 16:5520-5530.
73. Bamburg JR. Proteins of the ADF/cofilin family: essential regulators of actin dynamics. Annu Rev Cell Dev Biol 1999; 15:185-230.
74. Nagaoka R, Abe H, Obinata T. Site-directed mutagenesis of the phosphorylation site of cofilin: its role in cofilin-actin interaction and cytoplasmic localization. Cell Motil Cytoskeleton 1996; 35:200-209.
75. Carlier MF. Control of actin dynamics. Curr Opin Cell Biol 1998; 10:45-51.
76. Didry D, Carlier MF, Pantaloni D. Synergy between actin depolymerizing factor/cofilin and profilin in increasing actin filament turnover. J Biol Chem 1998; 273:25602-25611.
77. Moon A, Drubin DG. The ADF/cofilin proteins: stimulus-responsive modulators of actin dynamics. Mol Biol Cell 1995; 6:1423-1431.
78. Rosenblatt J, Agnew BJ, Abe H, Bamburg JR, Mitchison TJ. Xenopus actin depolymerizing factor/cofilin (XAC) is responsible for the turnover of actin filaments in Listeria monocytogenes tails. J Cell Biol 1997; 136:1323-1332.
79. Whitaker MJ, Steinhardt RA. Ionic regulation of egg activation. Q Rev Biophys 1982; 15:593-666.
80. Johnson CH, Epel D. Intracellular pH of sea urchin eggs measured by the dimethyloxazolidinedione (DMO) method. J Cell Biol 1981; 89:284-291.

FIGURE LEGENDS

Figure 1. (A) CASA motility parameters for stallion sperm suspensions after 30 min incubation with various concentrations of MitoTracker Green FM (MTG) dissolved in DMSO: 0 nM MTG, 200 nM MTG and 0.025% DMSO, 400 nM MTG and 0.05% DMSO, 800 nM MTG and 0.1% DMSO, 0 nM MTG and 0.05% DMSO and 0 nM MTG plus 0.1% DMSO and subsequently diluted in 10 ml non-capacitating medium. Bars show mean (± s.d.) percentages of motile (dark grey bars) and progressively motile (light grey) spermatozoa for three replicates. For the percentage of motile spermatozoa, values that differ significantly are indicated by different small letters (motile sperm) or capitals (progressively motile sperm). Comparisons were performed using repeated measure ANOVA with Greenhouse-Heisser and Bonferroni correction, followed by Scheffé post hoc tests for pairwise comparisons. (B) Fluorescence microscope images of spermatozoa stained with MitoTracker Green FM (MTG) dissolved in DMSO (a) 0 nM MTG, (b) 200 nM MTG and 0.025% DMSO, (c) 400 nM MTG and 0.05% DMSO and (d) 800 nM MTG and 0.1% DMSO. Corresponding light microscope images (e, f, g, h) were taken by DIC (original magnification, 1000 x: Bar = 25 μm).

Figure 2. Motility patterns indicative of hyperactivated motility were assessed by CASA and included (A) lateral head displacement (ALH) and (B) curvilinear velocity (VCL) in 200 nM MitoTracker Green (MTG) + 0.025% DMSO labelled (black bars) and non-MTG labelled (white bars) stallion sperm suspensions after 6 h incubation in capacitating medium and subsequently 30 min incubation in 0, 1, 2.5, and 5 mM procaine dissolved in capacitating medium (pH=7.4) (n=5 samples in each group; 3 replicates). Hyperactivated motility in sperm suspensions was clearly triggered by 2.5 and 5 mM procaine while motility indicative of hypermotility (ALH and VCL) was not evident at lower procaine concentrations. Pre-labelling stallion spermatozoa with MTG did not have any effect on hyperactivated motility. For both lateral head displacement and curvilinear velocity, values that differ significantly are indicated by different small letters. Repeated measure ANOVA with Greenhouse-Heisser and Bonferroni correction; Scheffé post hoc tests were performed for pairwise comparison. (C) The percentage of spermatozoa pre-labelled with 200 nM MTG dissolved in 0.025% DMSO (black bars) and 0 nM MTG (white bars) and subsequently incubated for 6 h in 0, 1, 2.5 and 5 mM procaine that showed tail-associated protein tyrosine phosphorylation was assessed at pH 7.4 and pH 7.9 (n=5 samples in each group; 3 replicates). Tail-associated protein tyrosine phosphorylation in stallion spermatozoa was cleary related to elevated medium pH 7.9 whereas procaine and MTG-DMSO did not have any effect. Values that differ significantly are indicated by different small letters. Repeated measure ANOVA with Greenhouse-Heisser and Bonferroni correction; Scheffé post hoc tests were performed for pairwise comparison.

Figure 3. Confocal microscope images of (a) a cumulus-free oocyte after 18 h co-incubation with spermatozoa in 5 mM procaine diluted in capacitating medium, and stained with Hoechst and Mitotracker Green FM to assess sperm penetration, (b) an oocyte activated parthenogenetically using ionomycin (negative control) and (c) an oocyte fertilized by ICSI (positive control). Corresponding light microscopic images (a', b', c') were taken by DIC. The formation of a second polar body and the presence of a spermatozoon inside the cytoplasm of oocytes incubated with sperm, in the presence or absence of procaine, was never observed. Indeed, the formation of pronuclei was a rare observation (<3%) in oocytes incubated with sperm. Light microscopic DIC images of (d) an oocyte after 18 h co-incubation with unlabelled sperm in 5 mM procaine, (e) an oocyte activated parthenogenetically using ionomycin (negative control) and (f) an ICSI-fertilized oocyte (positive control) after post-fixation lacmoid staining were also examined. Both methods of evaluation indicated that IVF in the presence of procaine induced neither fertilization nor normal parthenogenesis, but instead triggered DNA fragmentation (n=20 oocytes; three replicates; original magnification, 630 x: Bar = 25 μm. ST; sperm tail. PN; pronucleus. PB; polar body. F; condensed DNA fragments).

Figure 4. Percentage of completely or partially cumulus-denuded oocytes that had degenerated or cleaved after 2.5 days in culture following fertilization incubation in capacitating medium containing 0, 1, 2.5, or 5 mM procaine with or without spermatozoa. ICSI fertilized oocytes were used as a positive control for cleavage (hatched bar). In the presence of 2.5 and 5 mM procaine, oocytes cleaved up to the 8-cell stage. Cleavage was not observed for 1 mM procaine or capacitating medium (0 mM procaine). Data represent mean (± s.d.) percentages of oocytes after incubation in capacitating medium (black bars), 1 mM procaine in capacitating medium (dark grey bars), 2.5 mM (light grey bars) and 5 mM procaine (white bars); n=20 oocytes in each group, three replicates. Values that differ significantly ($p<0.05$) are indicated by different small letters for degenerated oocytes or capitals for cleavage. Values that differ significantly between completely and partially cumulus-denuded oocytes are indicated by Greek letters ($p<0.05$). The numbers of degenerated and cleaved oocytes were analyzed by binary logistic regression, with chi-square ($\chi 2$) tests performed for pairwise comparison.

Figure 5. Micrographs of embryo developmental stages (a, e and i: 2-cell; b, f and j: 4-cell; c, g and k: 8-cell; d, h and l: 16-cell; m: blastocyst) after oocytes were incubated for 18 h in 2.5 mM procaine in capacitating medium with or without sperm, and subsequently cultured in a DMEM/ F12 plus 10% FBS based medium. Oocytes that cleaved in the presence of procaine never developed further than the 8-16 cell stage. ICSI fertilized oocytes were used as positive control (original magnification, 400x: Bar = 20 μm).

Figure 6. Percentages of completely or partially cumulus-denuded oocytes that showed (1) degeneration, (2) meiosis I stage (MI), (3) meiosis II stage (MII), (4) 1 pronucleus (1PN), (5) 2 pronuclei (2PN), (6) 1 DNA fragment (1F) and (7) 2 DNA fragments (2F) after 24 h in fertilization incubation in capacitating medium containing 0, 1, 2.5, and 5 mM procaine with or without spermatozoa. In general, this experiment showed clearly that procaine-exposed oocytes rarely form pronuclei but instead exhibit condensed DNA fragments. Data represent mean (± s.d.) percentages of oocytes after incubation in capacitating medium (black bars), 1 mM procaine in capacitating medium (dark grey bars), 2.5 mM (light grey bars) and 5 mM procaine (white bars); n=10 oocytes in each group, three replicates. Values that do not differ significantly ($p<0.05$) within each type of DNA configuration are indicated by the same small letter, and values that do not differ significantly between cumulus-free and cumulus-intact oocytes are indicated by the same capital letter ($p<0.05$). The numbers of degenerated and cleaved oocytes were analyzed by binary logistic regression, with chi-square ($\chi 2$) tests performed for pairwise comparison.

Figure 7. Confocal micrographs to demonstrate the DNA of different embryo developmental stages (a, e and i: uncleaved oocyte; b, f and j: 2-3-cell stage; c, g and k: 5-6-cell; d, h and l: 8-16-cell and m: blastocyst) after incubation for 18 h in 2.5 mM procaine in capacitating medium with or without sperm, followed by culture in a DMEM/F12 plus 10% FBS based medium. Many cells contained no DNA, and the visible DNA was very condensed and fragmented. ICSI fertilized oocytes were used as positive control (original magnification, 400x: Bar = 20 μm).

Figure 8. Representative cytoplasmic calcium oscillations assessed using the ratiometric dye, fura-2 AM, in equine oocytes exposed for 6 h to (a) 2.5 mM procaine and (b) 5 μM ionomycin or for 16 h after (c) fertilization by ICSI. Procaine did not induce a cytoplasmic calcium rise in equine oocytes, whereas a single early cytoplasmic calcium rise was observed after exposure to ionomycin, and multiple calcium oscillations were evident after fertilization by ICSI (n=20 oocytes for the procaine group; n=5 oocytes for the ionomycin group; n= 15 oocytes for the ICSI group).

Figure 9. Cortical granule exocytosis was assessed by LCA-FITC staining in (a) mature oocytes; (b) 6 h after exposure to 5 μM ionomycin; (c) 6 h after ICSI; 6 h after exposure to (d) 0 mM, (e) 2.5 mM procaine and (f) 5 mM Procaine (n=10 oocytes in each group; three replicates). Corresponding light microscopic images (a', b', c', d', e', f') were taken by DIC. Procaine did not induce cortical granule

exocytosis but ICSI fertilization and ionomycin activation did. Moreover, in the procaine-activated oocytes, the cortical granules were present not only in the periphery of the oocyte cytoplasm but also more centrally (original magnification, 630x: Bar = 25 μm).

Figure 10. (a) Intracellular pH was assessed at 0, 1, 3 and 6 h using the ratiometric dye BCECF-AM in equine oocytes exposed to 0, 1, 2.5, 5 and 10 mM procaine in capacitating medium. Increasing procaine concentration was associated with an increase in cytoplasmic pH. Values are mean (± s.d.) BCECF-AM ratio in oocytes exposed to 0, 1, 2.5, 5 and 10 mM procaine (n=5 oocytes in each group; three replicates). Values that differ significantly are indicated by different small letters ($p<0.05$). Comparisons were performed by repeated measure ANOVA with Greenhouse-Heisser and Bonferroni correction; Scheffé post hoc tests were used for pairwise comparisons. (B) Changes in BCECF-AM fluorescence intensity in equine oocytes exposed to 0, 1, 2.5, 5 and 10 mM procaine in capacitating media for 1 h. A clear procaine concentration dependent fluorescence signal (indicating a pH rise) was observed (original magnification, 100x: Bar = 25 μm).

Figure 11. Cortical F-actin distribution as assessed by actin phalloidin-FITC staining in (a) mature oocytes and (b) ICSI-fertilized oocytes (18 h after ICSI), compared to oocytes exposed for 18 h to (c) 0 mM (capacitating), and d) 2.5 mM procaine (n=10 oocytes in each group; three replicates). Corresponding light microscopic images (a', b', c' and d') were taken by DIC. Exposure of horse oocytes to procaine was associated with depolymerization (reduced abundance) of F-actin (original magnification, 630x: Bar = 25 μm).

Figure 1

A

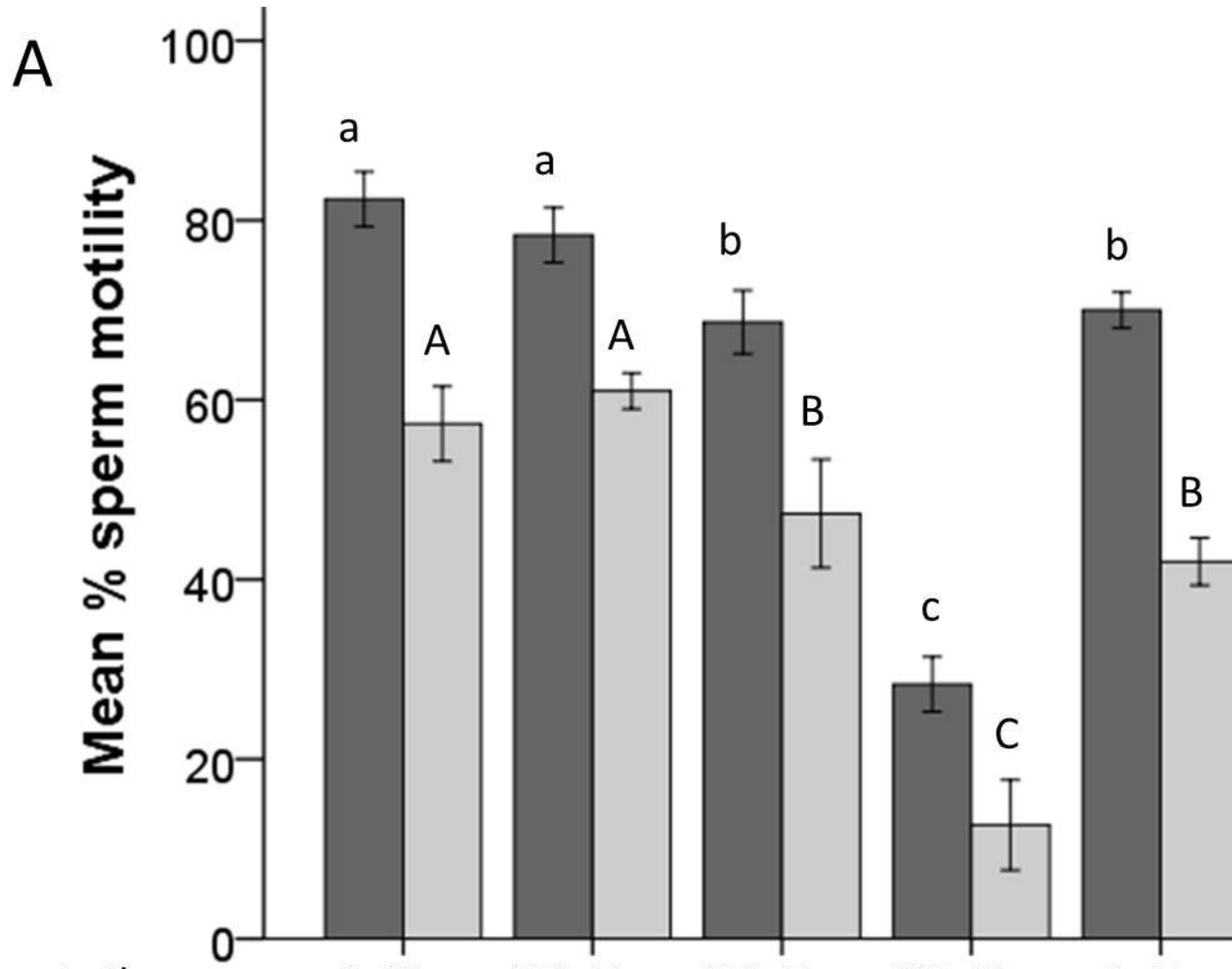

MT concentration:	0 nM	200 nM	400 nM	800 nM	0 nM	0 nM
DMSO:	0 %	0.025 %	0.05 %	0.1 %	0.05 %	0.1 %

B

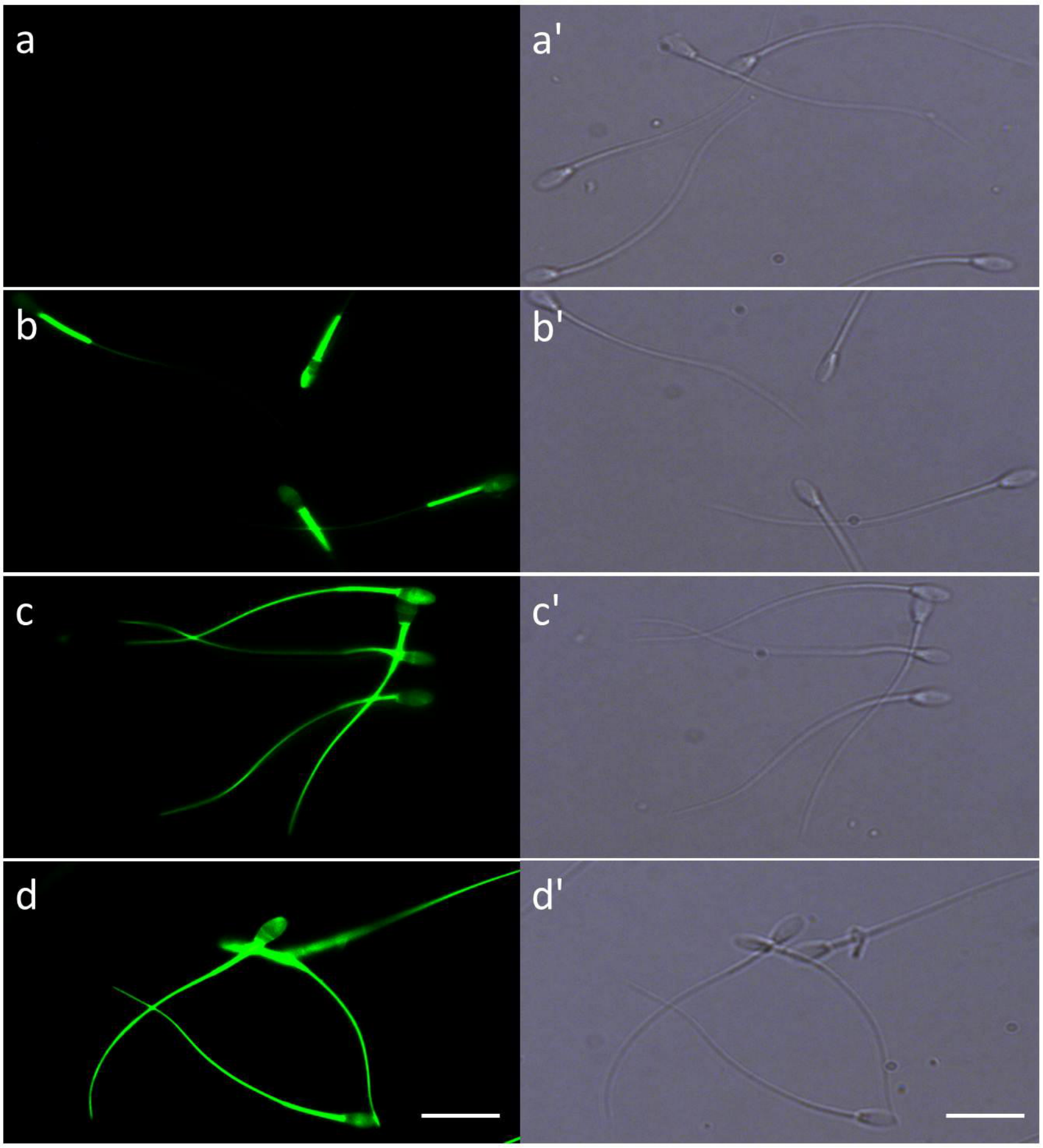

Figure 2

A

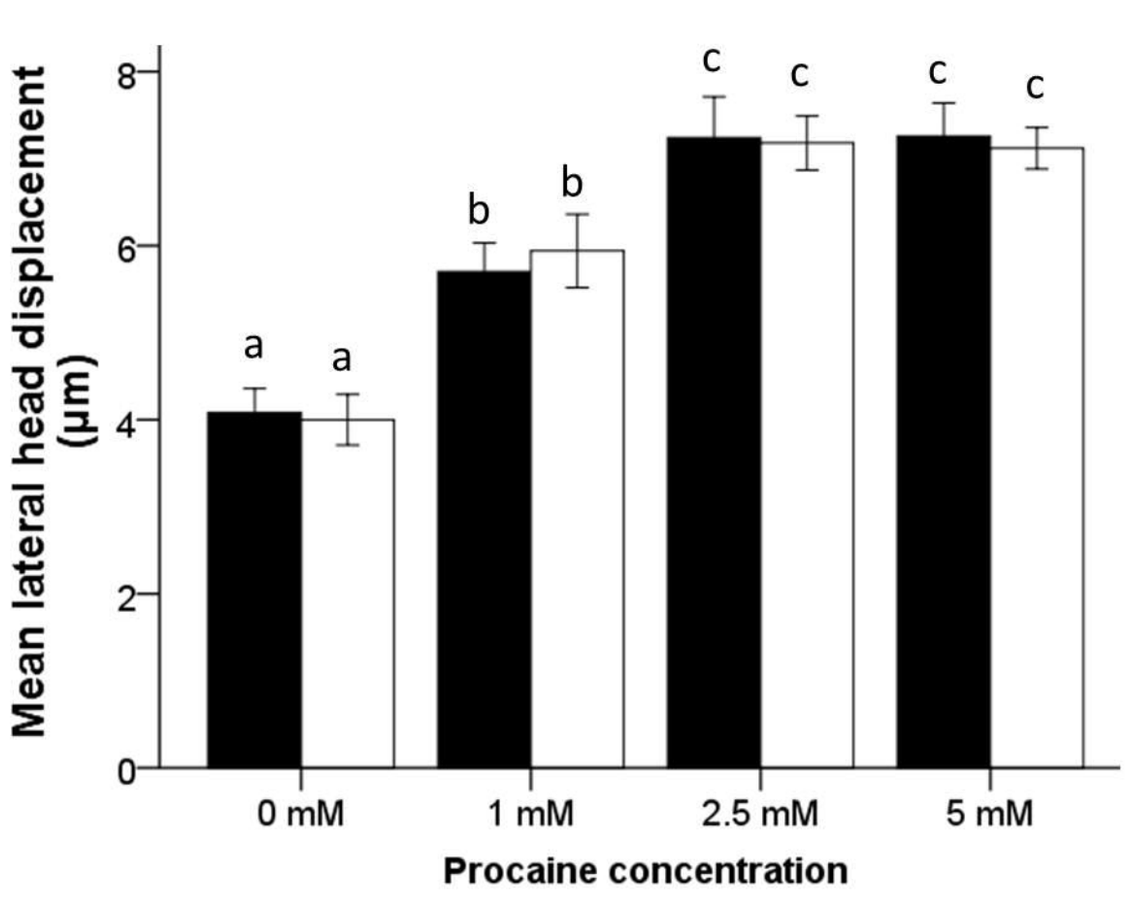
Mean lateral head displacement (µm)
0
2
4
6
8
a a b b c c c c
0 mM
1 mM
2.5 mM
5 mM
Procaine concentration

B

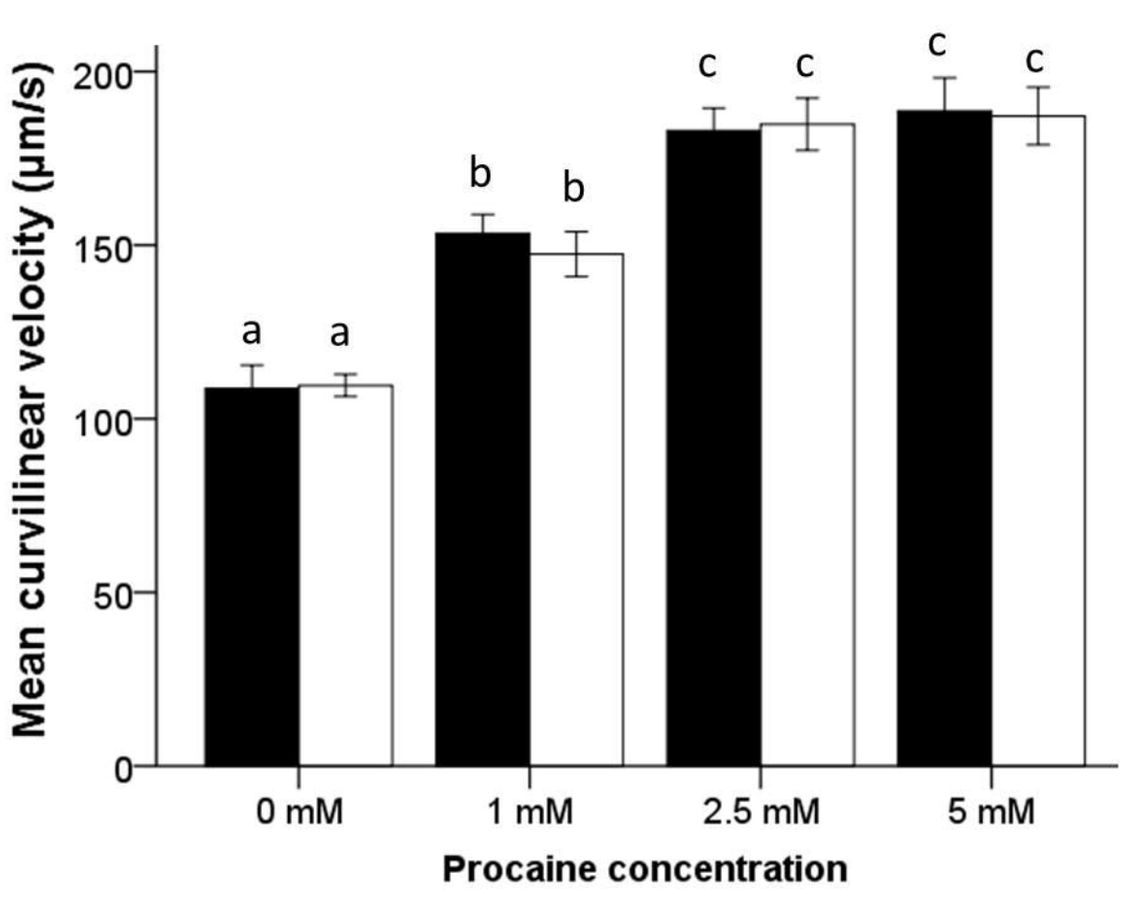
Mean curvilinear velocity (µm/s)
0
50
100
150
200
a a b b c c c c
0 mM
1 mM
2.5 mM
5 mM
Procaine concentration

C

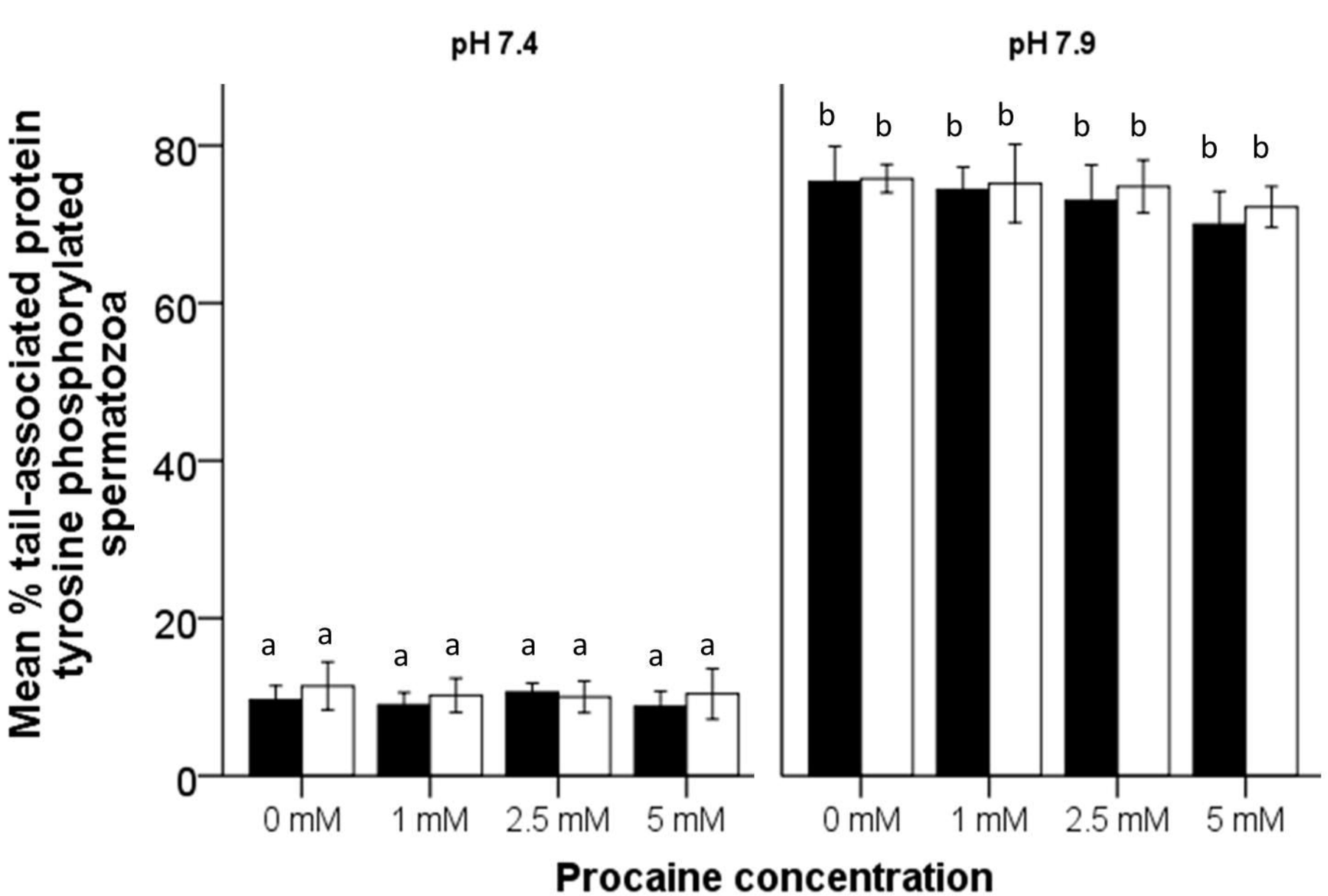
pH 7.4
pH 7.9
Mean % tail-associated protein tyrosine phosphorylated spermatozoa
0
20
40
60
80
a a a a a a a a
b b b b b b b b
0 mM
1 mM
2.5 mM
5 mM
Procaine concentration

Figure 3

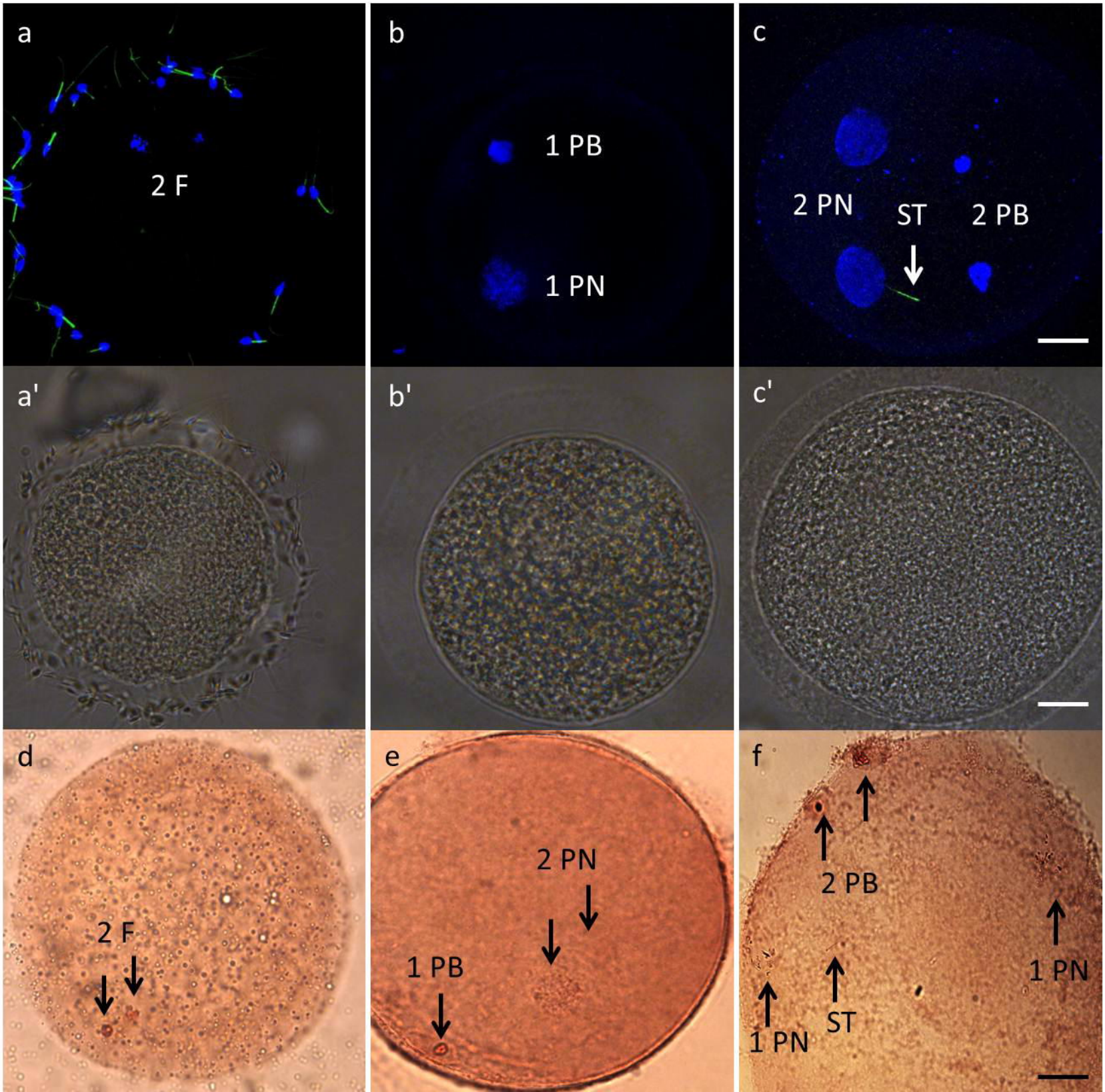

Figure 4

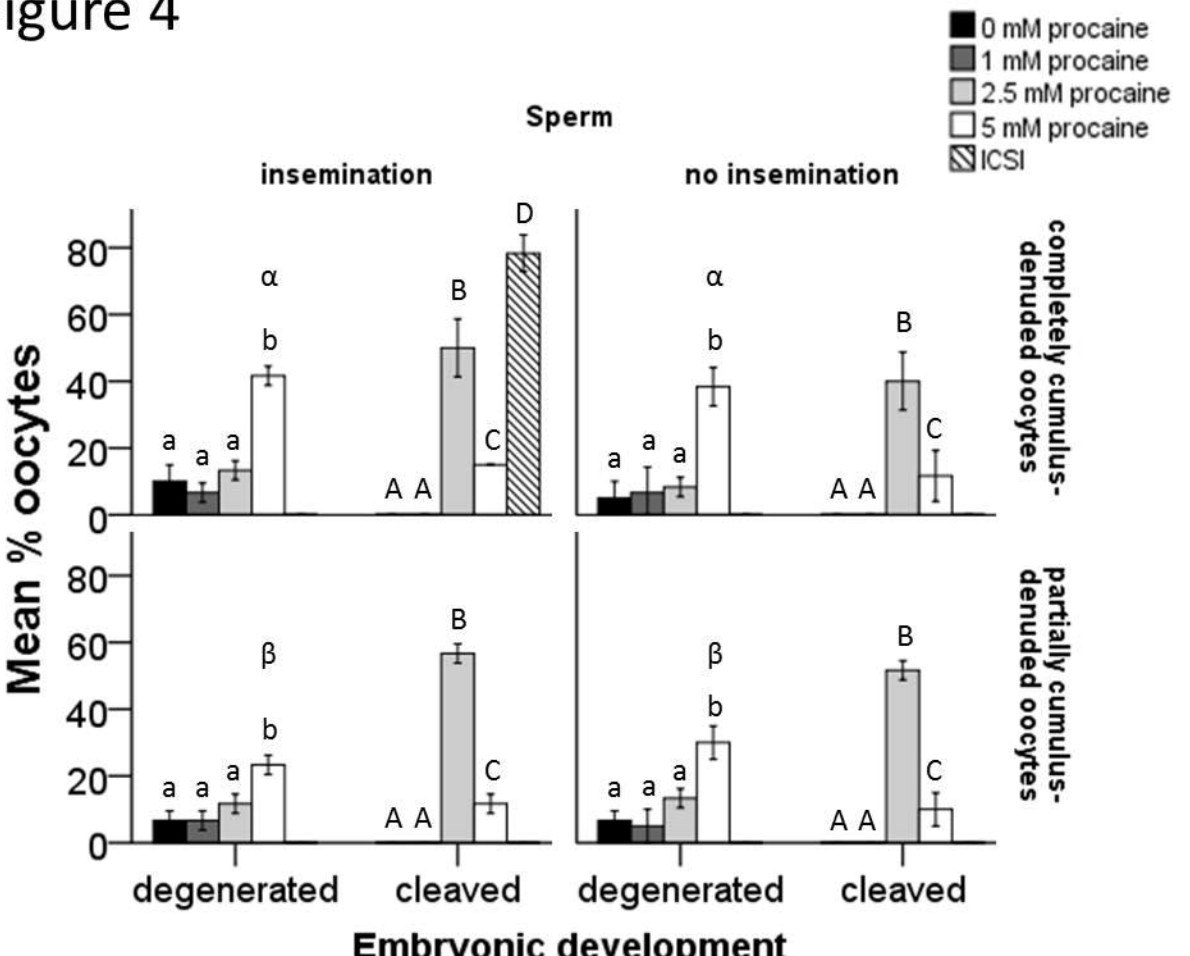
0 mM procaine
1 mM procaine
2.5 mM procaine
5 mM procaine
ICSI
Sperm
insemination
no insemination
completely cumulus-denuded oocytes
partially cumulus-denuded oocytes
Mean % oocytes
0
20
40
60
80
degenerated
cleaved
Embryonic development

Figure 5

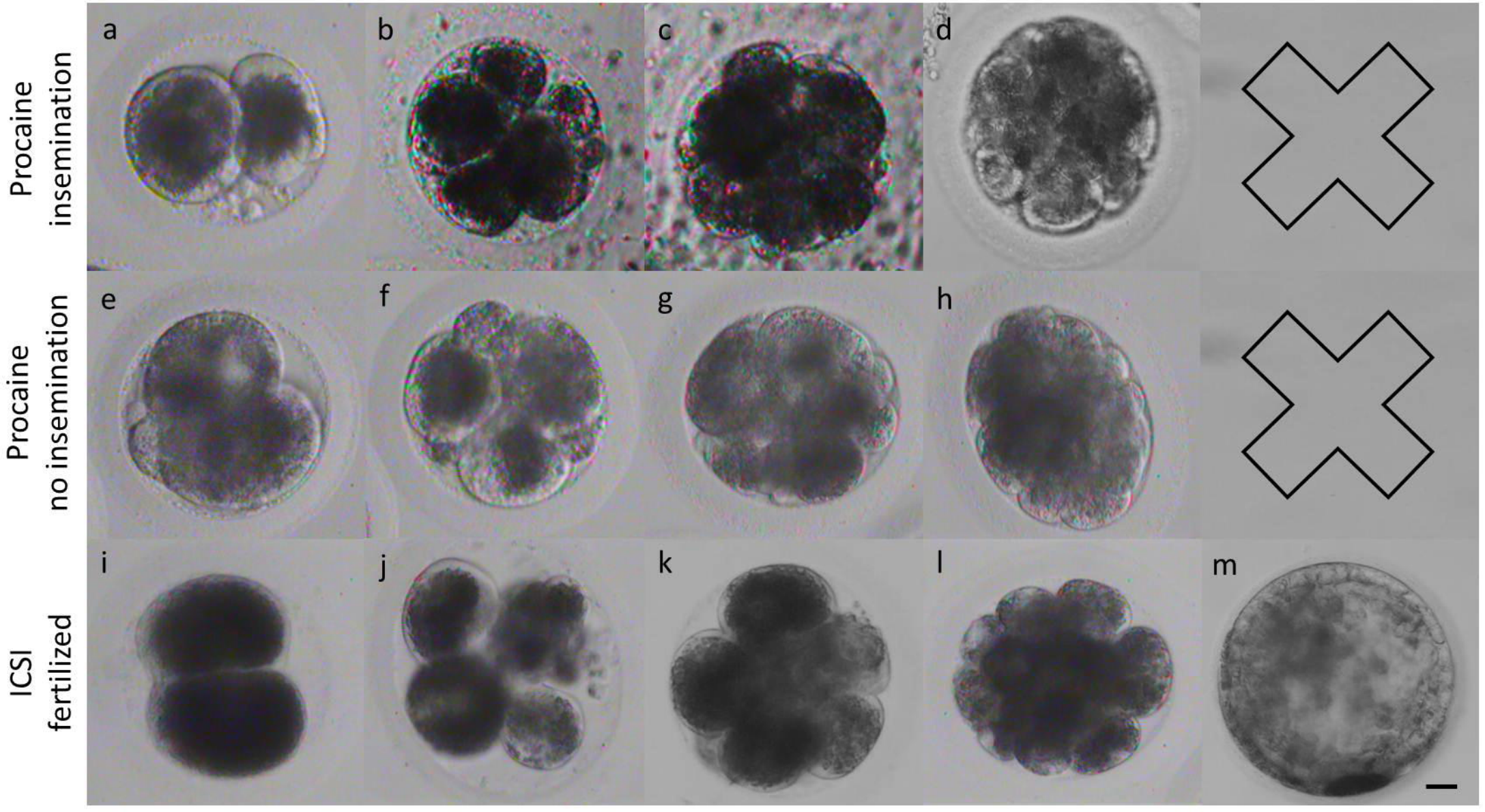
Procaine insemination
Procaine no insemination
ICSI fertilized
a
b
c
d
e
f
g
h
i
j
k
l
m

Figure 6

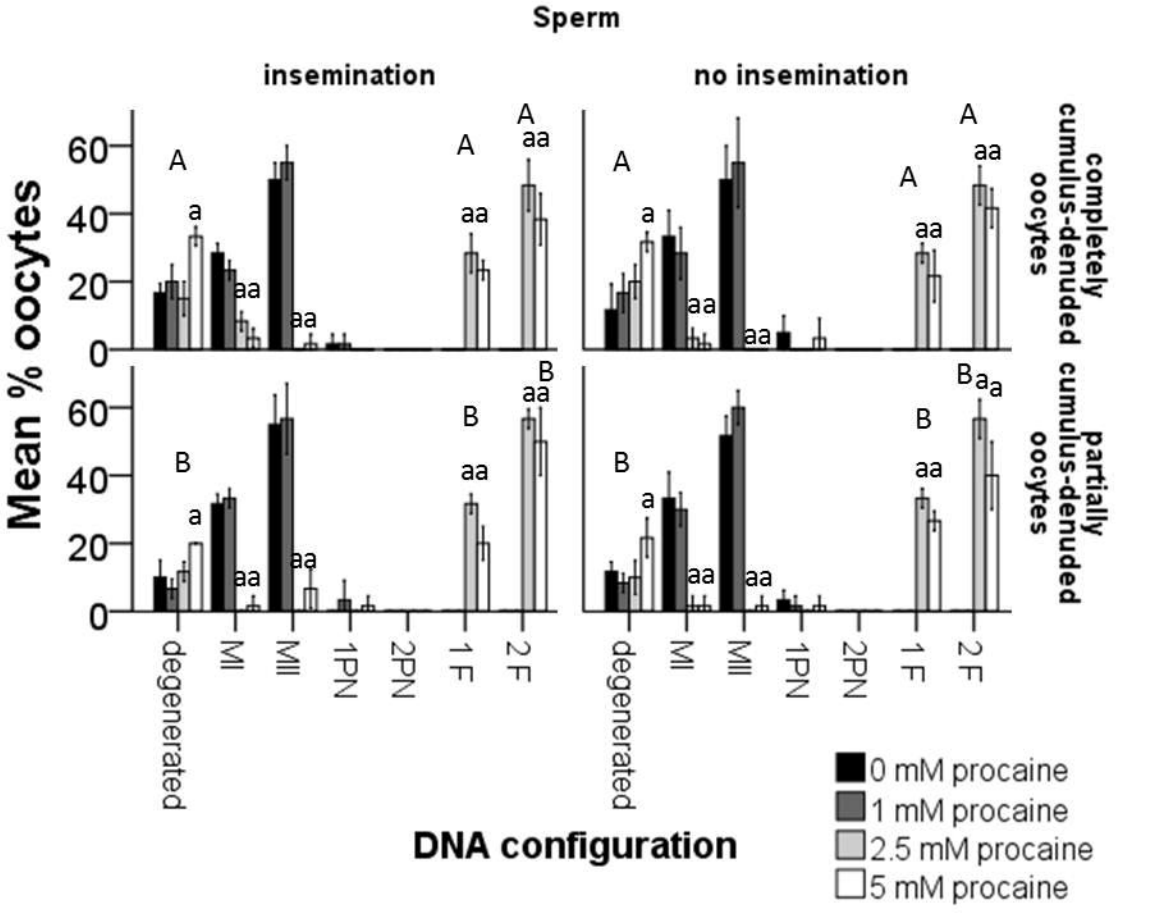
Sperm
insemination
no insemination
completely cumulus-denuded oocytes
partially cumulus-denuded oocytes
Mean % oocytes
0
20
40
60
degenerated
MI
MII
1PN
2PN
1 F
2 F
DNA configuration
0 mM procaine
1 mM procaine
2.5 mM procaine
5 mM procaine

Figure 7

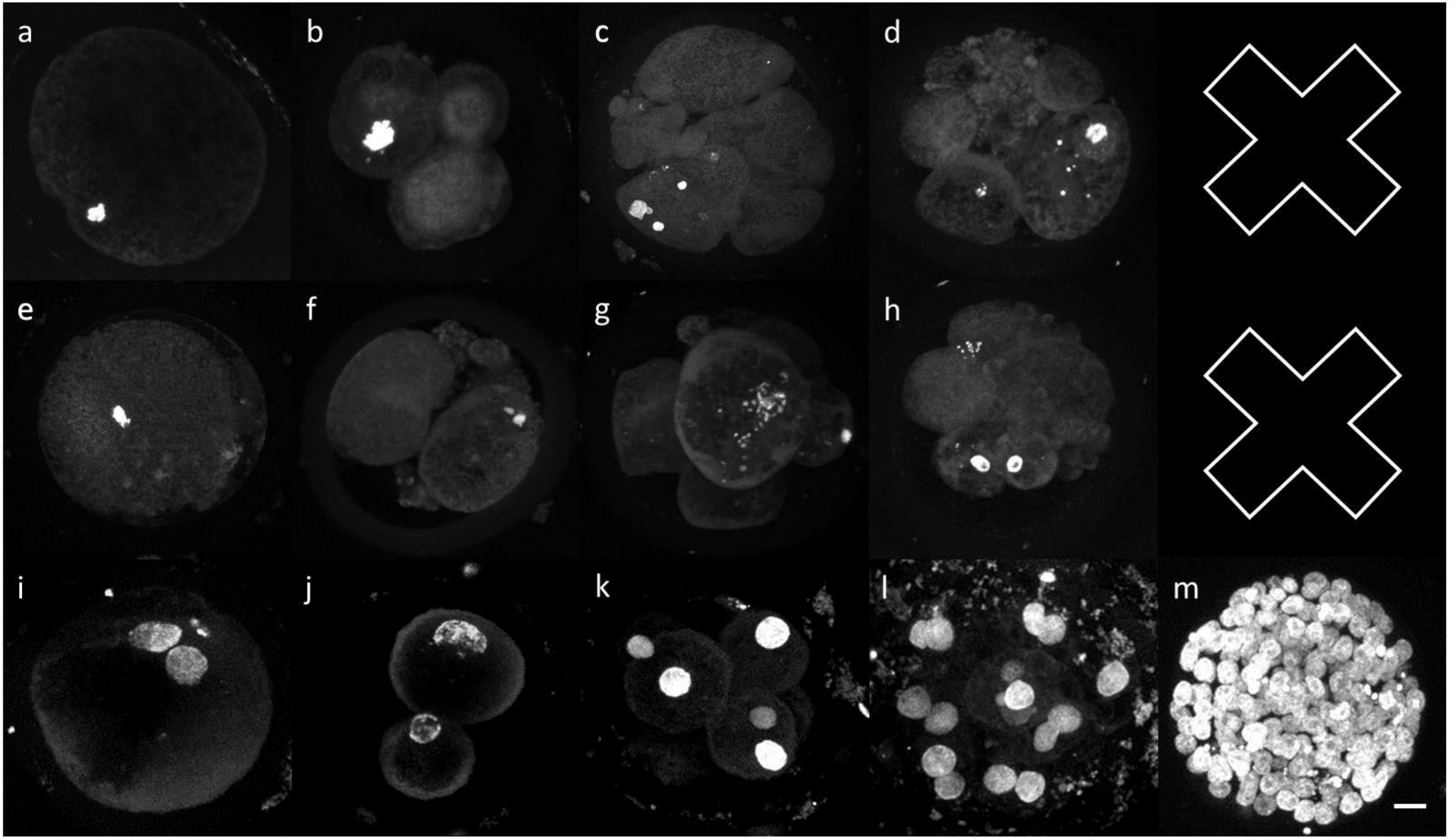
Procaine insemination
Procaine no insemination
ICSI fertilized
a
b
c
d
e
f
g
h
i
j
k
l
m

Figure 8

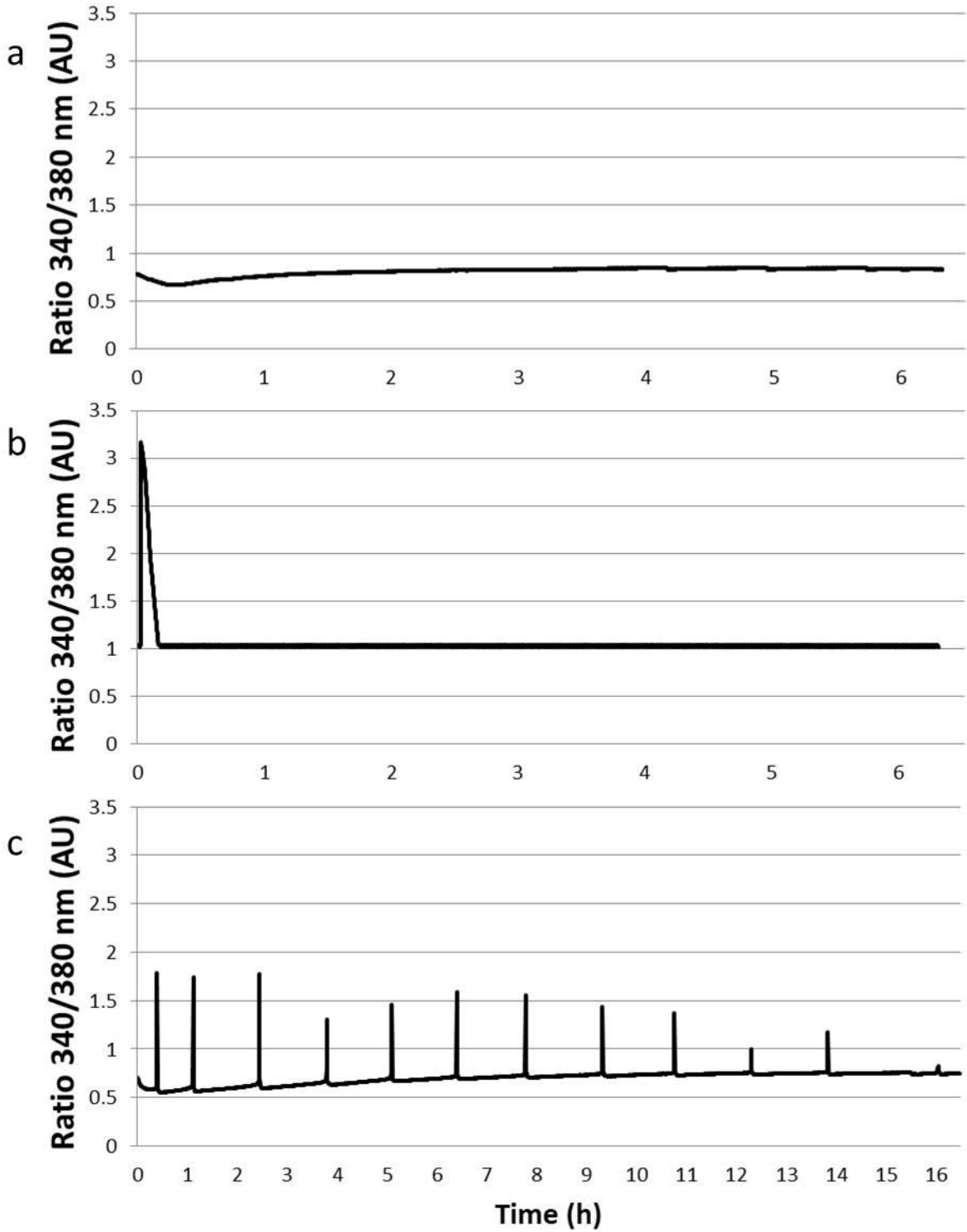
a
b
c
Ratio 340/380 nm (AU)
3.5
3
2.5
2
1.5
1
0.5
0
0 1 2 3 4 5 6
0 1 2 3 4 5 6 7 8 9 10 11 12 13 14 15 16
Time (h)

Figure 9

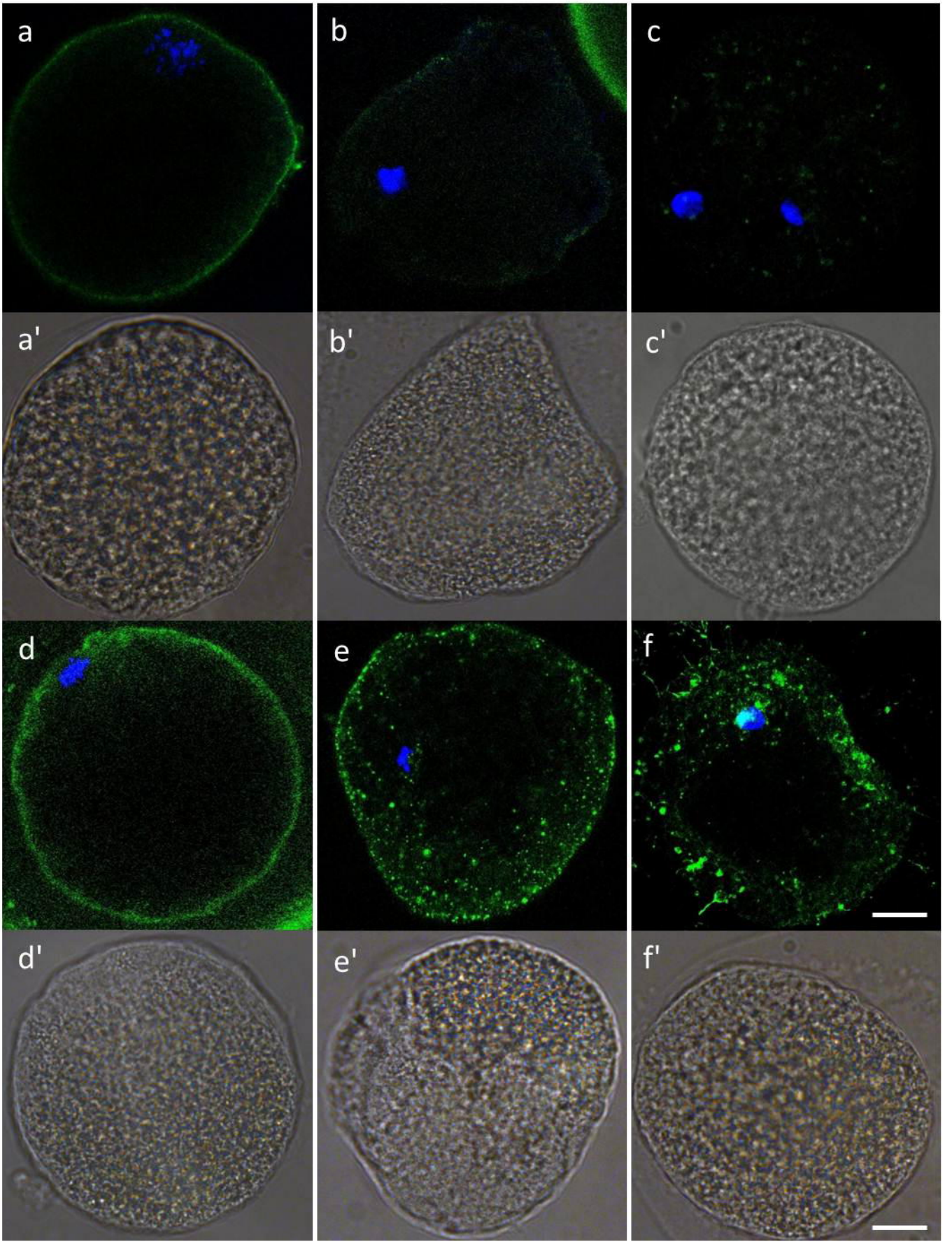

Figure 10

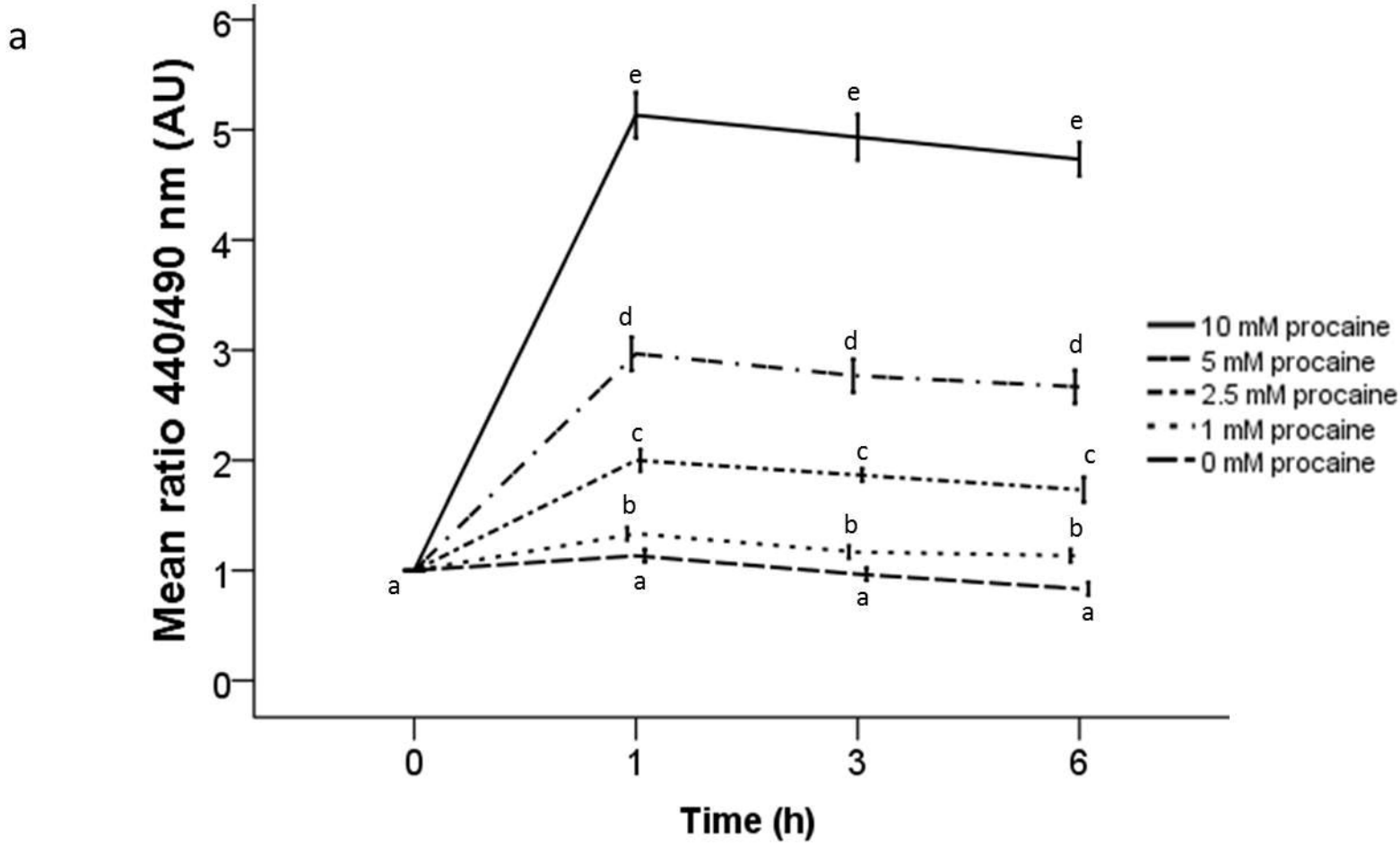
a
Mean ratio 440/490 nm (AU)
0
1
2
3
4
5
6
Time (h)
0
1
3
6
10 mM procaine
5 mM procaine
2.5 mM procaine
1 mM procaine
0 mM procaine
a
b
c
d
e

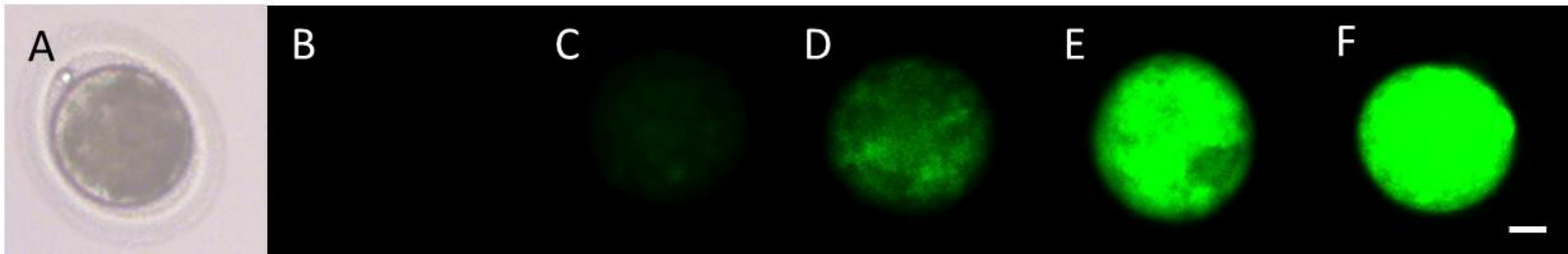
b
A
B
C
D
E
F

Figure 11